Chapter 26

Nanoscale, Catalyst Support Materials for Proton-Exchange Membrane Fuel Cells

Karthikeyan K. Karuppanan[1], Manoj K. Panthalingal[2] and Pullithadathil Biji[1,3]

[1]*Nanotech Research, Innovation and Incubation Centre, PSG Institute of Advanced Studies, Coimbatore, Tamil Nadu, India,* [2]*Department of Mechanical Engineering, PSG Institute of Technology and Applied Research, Coimbatore, Tamil Nadu, India,* [3]*Department of Chemistry, PSG College of Technology, Coimbatore, Tamil Nadu, India*

26.1 INTRODUCTION

The "fossil fuel depletion" became a great concern toward the end of the 20th century because of the alarming rate of increase in its usage and it also encompassed the issue of "global warming" since the main culprit is the CO_2 which gets emitted during the burning of any hydrocarbon fuel. The serious debates and discussions among the scientific community to solve these two issues have led to the identification of "the fuel for the future," viz., "H_2," the most abundant element in the universe. Hydrogen, which is not available freely in nature, exists in the form of water and in the form of hydrocarbons in plenty. Hydrogen being identified as the "future fuel," the next question was about the technology which could convert the chemical energy stored in the fuel to useful electrical energy. The conventional technology involves a three step conversion, viz., (1) chemical energy to heat energy by combustion process, (2) heat energy to mechanical energy using an engine, and (3) mechanical energy to electrical energy using a generator. The three-step conversion process limits the overall efficiency of conventional technology to less than 30%. The Fuel Cell Technology which involves the direct conversion of chemical energy of the fuel into useful electricity by electrochemical means has efficiencies of the order of 50% due to its single-step conversion. This very high efficiency of the fuel cell makes them a strong candidate for the chemical energy conversion of hydrogen into electrical energy. Hence, a lot of interest was shown by the scientific community on this technology by the end of the last century and a lot of research has taken place resulting in lots of publications and patents up to now.

The fuel cells are similar to batteries in their construction and their working. Both of them directly convert the chemical energy into electrical energy by electrochemical means. Similar to batteries, a fuel cell also has two electrodes and an electrolyte connecting them. The nomenclature of the fuel cells basically comes from the type of electrolyte which is used in that particular fuel cell. Based on the type of electrolyte used, fuel cells are classified as shown in Table 26.1.

Based on the temperature of operation they also can be classified as high, medium, and low temperature fuel cells. Lots of interest is shown in the development of proton exchange membrane fuel cells (PEMFCs) due to the solid nature of the fuel cell and the low operating temperature which makes the handling of such cells much easier.

26.2 PROTON EXCHANGE MEMBRANE FUEL CELL

PEM fuel cells get their name because the electrolyte used in such cells is a membrane which has the unique property of conducting protons through it. Due to its low temperature operation ($<80°C$) they are suitable for quite a lot of applications, viz., portable, stationary, and automobiles. Since the entire fuel cell is made of solid components the handling of PEM fuel cells is much easier. The main components of a PEM fuel cell are

1. *Proton exchange membrane (PEM):* A proton exchange membrane acts as the electrolyte in such fuel cells. It is made up of perflurosulfonic acid ionomer which gives the unique ability to conduct H^+ ions through it. It acts as a good electrical insulator and also prevents the gases to pass across it. The membrane should be always in hydrated state for the ionic conductivity to happen.

Handbook of Nanomaterials for Industrial Applications. DOI: https://doi.org/10.1016/B978-0-12-813351-4.00027-4

© 2018 Elsevier Inc. All rights reserved.

TABLE 26.1 Fuel Cell Types

Name of the Fuel Cell	Electrolyte	Operating Temperature (°C)
SOFC	Yttria-stabilized zirconia	600–1000
MCFC	Potassium/sodium carbonates in molten form	500–700
PAFC	Phosphoric acid	170–200
AFC	Potassium/sodium hydroxide	80–100
PEMFC	Proton exchange membrane	50–80

SOFC, solid oxide fuel cell; *MCFC*, molten carbonate fuel cell; *PAFC*, phosphoric acid fuel cell; *AFC*, alkaline fuel cell; *PEMFC*, proton exchange membrane fuel cell.

2. *Catalyst:* The best catalyst for the anodic and cathodic reactions in a PEM fuel cell is the platinum supported on carbon. Almost half the cost of a single fuel cell is due to the costly platinum that is used as catalyst. The support material ensures that the platinum catalyst is uniformly distributed across the entire catalyst layer and also the electrons that are formed during the electrochemical reaction are also carried away from the reaction site for further reactions to occur.
3. *Carbon electrodes:* Porous carbon either as paper or as cloth is used as electrodes on both cathode and anode side of the fuel cell. They are also known as "gas diffusion layer," as they have to uniformly distribute the gas over the entire catalyst layer. They also need to conduct electrons and also need to carry away the heat that is generated during the electrochemical reactions. They are made hydrophobic in order to take away the liquid water formed during the continuous operation of the fuel cell. The electrolyte membrane, the catalyst layers, and the carbon electrodes are hot pressed together to form a single unit called membrane electrode assembly (MEA).
4. *Flow field plates:* The flow field plates are made of graphite and have flow channels machined on them for the hydrogen and oxygen gas to flow through them. The flow channel designs used help in uniformly distributing the reactants over the entire active area of the fuel cell at minimum pressure drop. The flow channels also have a big role to play in the water management inside the fuel cell. The graphite plate also helps in conducting away the heat produced during the operation of the fuel cell.
5. *Current collector plates:* Copper plates with gold coating are used for current collection. The current is drawn from the fuel cell through these plates for powering the devices.
6. *End plates:* The end plates made of aluminum are used to hold the entire fuel cell assembly together using bolts and nuts.

A single cell gives an open circuit voltage of around 1 volt and while extracting power the cells typically operate at voltages of 0.5–0.6 V. In order to power devices requiring higher voltages, the cells are connected in series so the voltage gets added up. The unit consisting of single cells connected in series is called the "stack." The working principle of the PEM fuel cell is the reverse of water electrolysis. Water gets separated into hydrogen and oxygen and gets evolved at the electrodes by the supplied of an electrical potential to the electrodes in water electrolysis. Hydrogen and oxygen are supplied to the respective electrodes and electrochemically combined together producing an electric potential in a PEM fuel cell. The anodic and cathodic reactions in PEM fuel cells are

$$H_2 \rightarrow 2H^+ + 2e^- \tag{26.1}$$

$$2H^+ \frac{1}{2}O_2 + 2e^- \rightarrow H_2O \tag{26.2}$$

The performance and the cost of the PEM fuel cell are mainly dependent on the catalyst used in the fuel cell. Even though a lot of research is going on in developing an alternate to platinum catalyst, platinum continues to be the best catalyst at present. Effective utilization of the platinum catalyst is another area in which a lot of studies are being carried out at present, in which the support material for the platinum catalyst has a big role to play.

26.3 TRIPLE PHASE BOUNDARY

In general, the hydrogen oxidation reaction (HOR) and oxygen reduction reaction (ORR) occur only at confined spatial sites, called triple phase boundaries (TPBs). The TPB of a fuel cell is the region of contact between the three phases necessary for electrochemical reactions at the electrode: ion conducting phase, electron conducting phase, and gas phase [1]. A simplified schematic diagram representing the TPB is shown in Fig. 26.1. Quantification of active TPBs is important in terms of the

determination of the structure and composition to yield maximum electrochemical performance of PEM fuel cells. Several methods and models have been introduced to increase the number of three phase boundary sites. Centi et al. introduced defects on carbon nanotubes (CNTs) by ball milling method. The Pt nanowires were grown on carbon cloth from an aqueous solution of H_2PtCl_6 and formic acid at room temperature followed by ionomer deposition using THF solution of Nafion (Fig. 26.1) [2].

The gas diffusion layers (GDLs) were tested as cathodes in a 25 cm^2 at 65°C and durability of the prepared material was studied by Du et al. [3]. Wang et al. developed an MEA with incorporation of porous polytetrafluoroethylene (PTFE) matrix. The electrochemical active area was increased at the cathode side due to the porous structure of the PTFE matrix. The electrochemical studies showed three-fold increase in cathode electrochemical surface area (ECSA) leading to improved catalytic activity. The overall performance of the cell was found to be 20% higher than typical MEAs. Fig. 26.2 shows an expanded view of the embedded PTFE matrix within the MEA [4,5] mixed Nafion solution and nanoporous SiO_2 and the prepared solution was coated between the electrode and solid electrolyte. The nanoporous SiO_2 was acting as a self-humidifying agent and the coated layer between electrode and solid electrolyte expanded three-dimension electrochemical reaction area. This also improves the back-diffusion of water from cathode to anode, so that the total performance also increased the power density 1.5 W/cm^2 under 0.2 MPa.

26.4 CATALYST MATERIALS USED IN PEM FUEL CELLS

The most common catalyst used in commercial PEM fuel cells is platinum nanoparticles dispersed in carbon materials. Conventionally, platinum salts are reduced chemically using a reducing agent for the synthesis of Pt catalyst materials. Subsequently, these particles are adsorbed by a high-surface area carbon to make a Pt/C powder [6] which allows for the reactions between hydrogen and oxygen. So far, Pt-based materials are the best-performing

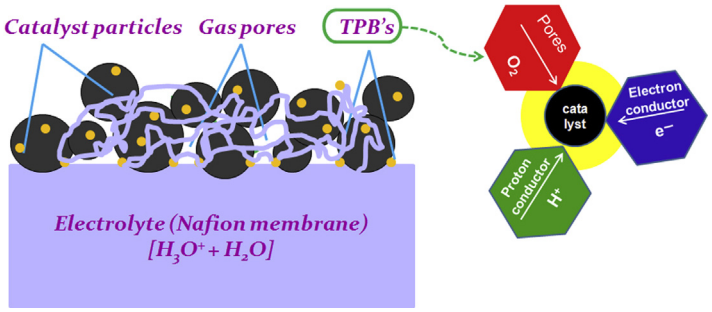

FIGURE 26.1 A schematic diagram of triple phase boundary model.

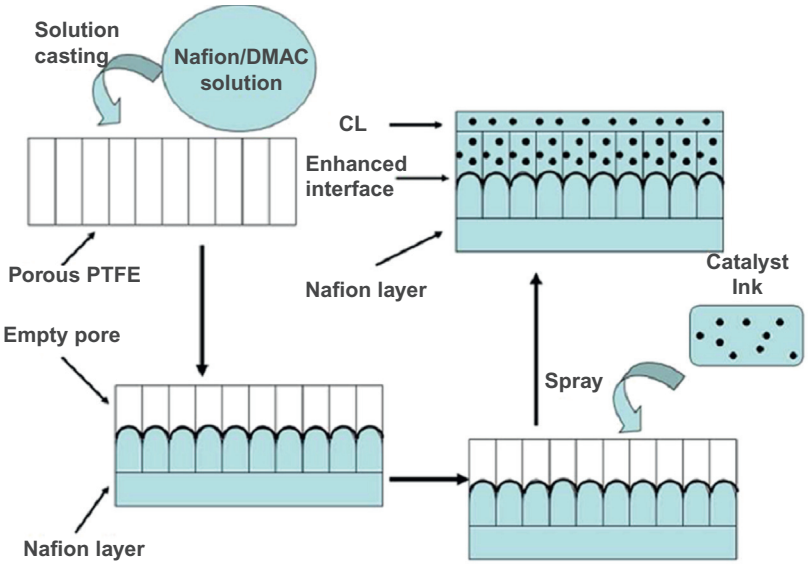

FIGURE 26.2 A scheme of preparation method for the MEA with enhanced membrane/electrode interface. *MEA*, membrane electrode assembly. *Reprinted from L. Wang, S.G. Advani, A.K. Prasad, Membrane electrode assembly with enhanced membrane/electrode interface for proton exchange membrane fuel cells, J. Phys. Chem. C, 117, (2013), 945–948. ©2013 American Chemical Society.*

catalysts for both anode and cathode of PEM fuel cells. The first-generation Pt catalyst was Pt black. A large quantity of catalyst was required to generate substantial power output in a cell. For better operating efficiency, catalysts are now made of nanoparticles supported on carbon black or CNTs. There are some commonly used methods to prepare Pt (or Pt alloy)/C catalysts. In wet-chemical method, Pt and other metal nanoparticles are prepared by a reduction reaction in a solution containing salts of these metals. Carbon supports (carbon black with high surface area or CNTs) are dispersed into the sol and metal nanoparticles adsorb onto the carbon surface. After washing, drying, and reducing in H_2 (depends on metal type), nanocatalysts having diameter $\sim 3-4$ nm can be obtained [7,8]. In situ reduction also is found to be a very efficient method, where carbon supports are first dispersed in salt solution, and then a reducing agent is introduced into this hot suspension dropwise. Grigoriev et al. [9] used ethylene glycol and formaldehyde as reductants to reduce H_2PtCl_6 in a suspension of Vulcan XC-72. The Pt nanoparticles were deposited onto carbon nanoparticles during reduction. Rajalakshmi et al. [10] developed Pt/multiwalled CNTs (MWCNTs) catalyst by dispersing CNTs into H_2PtCl_6 solution. $NaBH_4$ in the presence of NaOH was used to reduce Pt salt. Plasma sputtering is another physical method used to deposit a Pt layer. Caillard et al. [11] reported sputtering of platinum onto carbon nanofibers (CNFs), which resulted in the formation of nanoclusters (3−8 nm) on the periphery of the CNFs. Microwave-assisted polyol process can be employed to synthesize carbon-supported Pt catalysts for fuel cells. In a study by [12], a polyol (ethylene glycol) solution containing catalyst precursor salt, H_2PtCl_6 and carbon support was irradiated in a microwave for 60 seconds. Pt/C catalyst was synthesized with uniform sized (3.5−4 nm) Pt nanoparticles. Gruber et al. [13] used sputtering method to deposit Cr as a sublayer for Pt coating. Addition of a thin layer of chromium underneath the catalyst layer showed an improved performance due to its change in morphology. Pd−Co−Mo ternary alloy catalyst was prepared by [14] for PEMFC. The catalytic activity was compared with Pt, Pd−Co−Au, and Pd−Ti which resulted in an optimum composition of Pd:Co:Mo = 70:20:10 and exhibited improvement in catalytic activity. A sequential reduction method was followed by [15] to prepare Fe_2O_3@Pt core shell nanoparticles on carbon support. This study proved that the catalyst effectiveness depends mainly on the thickness of the catalyst material deposited. Crossing the thickness beyond a threshold level disturbs the electrochemically active surface area, oxygen reduction kinetics, and polarization characteristics. Nanowire network of platinum were synthesized by [16] via chemical reduction of a platinum complex in the presence of a template formed by cetyltrimethylammonium bromide in a water-chloroform two-phase system. Lee et al. [17] fabricated nanoscale platinum fibers via electrospinning Pt precursor/polymer composite fibers followed by subsequent thermal annealing. The conductivity of synthesized Pt nanofibers was found to be $\sim 10^4$ S/cm, which showed an improved conductivity than bulk Pt. Ahn et al. [18] fabricated a 3D nanostructured CNT array/PtRu nanoparticles for micro fuel cells. Improved catalytic activity and stability was observed in methanol electro oxidation. In order to overcome agglomeration issues [19], prepared surfactant free gold ultrafine clusters and other metal clusters (Pt, Pd) on reduced graphene oxide (rGO) without any shielding molecule and reductants for cathode catalysts. An uniform dispersion of particles were found on the graphene flakes and the electrocatalytic activity of the as-synthesized Au cluster, Pt, Pd/rGO were compared with same size of Pt/C, rGO sheets, Au nanoparticle/rGO hybrids, and thiol-capped Au clusters, which showed a comparable onset potential to Pt/C catalyst and superior stability. Zhao et al. [20] produced Pt and Pt−Ru nanowire (~ 30 nm) array electrodes by electrodeposition of Pt and Ru into the pores of an anodic aluminum oxide template on a Ti/Si substrate [21,22]. Most often, template method was used to make Pt wires. Zhang et al. [23] performed an electrodeposited Pt−Cu alloy nanowire in nanochannel alumina templates and dealloyed the Cu component, to make porous Pt nanowire arrays. An enhancement in electrocatalytic activity and stability was found in these porous nanowire nanostructure Pt electro-catalysts. By using nanoimprint lithography an orderly arrays of Pt nanowires having controlled diameter and length, with dimensions of 20-nm width, 5-nm height, and 12-μm length on planar oxide thin films of silica, alumina, zirconia, and ceria were produced by [24]. Peng et al. developed an *N*-doped carbon catalyst along with graphene for ORR. The ORR performances of the catalysts were evaluated electrochemically. The MEAs with an active area of 5.0 cm^2 were fabricated using the catalyst-sprayed membrane and its performance was checked. The catalyst shows high stability after 10,000 cyclic voltammetry cycles and showed maximum power density of 0.33 W cm^2 at 0.47 V. Peng et al. and Choi et al. [25,26] fabricated platinum nanowires using template method by electrodeposition of platinum within pores of a track-etched polycarbonate membrane. These wires showed an improved electrochemical methanol oxidation than supported or unsupported Pt nanoparticles with high loading of Pt. Lu et al. [27] synthesized platinum nanowires on CNTs templates through sonochemical method with the diameters of 60−70 nm. The limitation of these wires was their large diameter, which caused increased Pt mass utilization. Zhou et al. [28] fabricated a one-dimensional metal nanowire crystals using surfactant, ambient, free

synthesis technique. Pt nanowires had a higher ORR activity as compared with that of Pt nanoparticles. Teng et al. [29] synthesized bimetallic $Au_{48}Pt_{52}$ and $Au_{25}Pt_{75}$ nanowires with heterogeneous structure having average length of 100 nm and average diameter of 2.6 nm via wet chemistry approach. Xie et al. [30] suggested a template-free synthetic route for production of porous Pt nanocrystals. The structure could be spheres, rod-shaped, knot-shaped, and so on. Chen et al. [31] reported the synthesis of Pt nanotubes (PtNTs) and Pt−Pd nanotubes by galvanic replacement reaction of silver nanowires. ECSA of the PtNTs decreased about 20% after 1000 cycles in the durability test, while the platinum-black and Pt/C catalysts lost about 51% and 90% of their platinum ECSA, respectively. The increase in platinum nanoparticle size from 2−5 to 10−20 nm was the primary cause of platinum ECSA loss in the Pt/C catalysts. So it was identified that the supportless one-dimensional structure of Pt wires made them considerably more durable than zero-dimensional Pt nanoparticles. Fenske et al. [32] made short length Pt nanowires by aggregation of quasispherical particles. The nanowires obtained had a diameter approximately 2 nm and a length of 20−50 nm. The nanowires were found to be stable up to 140−160°C. Lee et al. [33] prepared Pt and W supported Pt nanorods by direct growth along the ⟨1 1 1⟩ axis on the surface of Pt or W gauze. These Pt nanowires supported on Pt gauze showed an enhanced electrochemically active surface area with improved activity toward the methanol oxidation reaction. Chen et al. inferred that the addition of a small amount of iron species (Fe^{2+} or Fe^{3+}) to the polyol process could notably alter the reduction kinetics of a Pt precursor and subsequently induce the Pt nanorods formation. Sun et al. [34] developed a wet-chemical procedure to synthesize single-crystal Pt nanowires and their flower-like assemblies on carbon black via reduction of hexachloroplatinic acid by formic acid (HCOOH) at room temperature which showed 50% higher mass activity than the commercial cathode.

26.5 CATALYST SUPPORT MATERIALS

Platinum is the most commonly used catalyst material for ORR and HER reactions occurring in PEMFCs, but, the high cost and low natural abundance of this noble metal hinders the large-scale commercialization of this technology. To reduce the quantity of platinum, various support materials with excellent physical and structural properties have been investigated. In order to bring down the cost of material, many researchers have focused their attention in obtaining high catalytic activity and catalyst utilization. In addition, uniform dispersion of the catalyst particles on the porous support material is an important requirement for the catalytic activity improvement. In general, the fuel cell commercial electrocatalysts are prepared by dispersing catalyst nanoparticles (2−5 nm) on carbon supports. An ideal catalyst support material must meet the important requirements of large specific surface area, mesoporous structure, electronic conductivity, water handling ability to avoid flooding, high electrochemical stability in acidic or alkaline medium, and easy recovery of electrocatalysts to improve the catalytic efficiency and catalyst loss [35]. The following sections describe the development of recent advances in inorganic metal oxide-based catalyst support materials as well as carbon-based support materials, such as graphite nanofibers, graphene, CNTs, and mesoporous carbon etc., used in PEMFCs.

26.6 NONCARBONACEOUS AND INORGANIC CONDUCTIVE OXIDE/CARBIDE SUPPORTS

Many conductive or semiconductive oxides and carbides have been studied as catalyst supports to address the activity and durability issues. The noncarbonaceous oxide supports such as TiO_x, WO_x, SnO_2, SiO_2, indium-doped tin oxide (ITO) are considered as more appropriate materials for this application due to their inertness in strong oxidative conditions [36−40]. The following sections give an account of various noncarbonaceous: metal oxide/carbide/boride and hybrid support materials of PEMFCs which have gained a lot of attention during the last few years.

26.7 TITANIUM OXIDE

Titanium oxide or titania (TiO_2) materials are regarded as the most extensively adopted conductive metal oxides due to their outstanding corrosion resistance in different electrolyte media. The high electrochemical stability and corrosion resistance established by these oxides have the potential to perform as catalyst supports in fuel cells [41,42]. Additionally, TiO_2 is an easily available, low cost, and nontoxic material that can mainly exist in three different forms such as, rutile, anatase, and brookite [43]. Anatase titania is identified as a more efficient photocatalyst compared to rutile structure. Typically, stoichiometric titania (band gap 4.85 eV) is resistive and the occurrence of Ti^{3+} ions is necessary for improving electronic conductivity. Ti^{3+} ions can be produced by subjecting TiO_2 into heat in a reducing environment to create oxygen deficiency (to obtain TiO_{2-x} or Ti_nO_{2n-1}) or by adding dopants in the lattice. For instance, Ti_4O_7 shows higher electrical conductivity of 1000 S/cm at room temperature than graphitized carbon (727 S/cm) [44,45]. In addition to that, these oxides have high electrochemical stability in acidic condition. Furthermore, the presence of labile

protons in the titanium oxide indicates the pronounced proton conductivity, hence these mixed electronic and protonic conductivity can be more favorable for the formation of the electrochemical TPB [46,47]. However, when it is exposed to fuel cell condition, substoichiometric titania becomes stoichiometic and forms a resistive TiO_2 layer at the three-phase reaction interface [48,49]. Huang et al. synthesized Pt (3−5 nm) supported on high surface area (266 m^2/g) mesoporous TiO_2 (7−15 nm) using a template-assisted method as an electrocatalyst for PEMFC cathode. Their accelerated degradation test (ADT) revealed higher ORR performance and high durability for Pt/TiO_2 compared to commercial Pt/C (45.9 wt.% TKK) [36]. Similarly, an optimal concentration of Pt/Pd (70:30) electrocatalysts on TiO_2 support material was prepared and studied for electrochemical activity by Huang et al. [50]. Kim et al. [51] evaluated the ORR activity by studying the effect of additives on TiO_2 as support for Pt electrocatalyst. They modified the electronic characteristics of TiO_2 supports with various additives, such as urea, thiourea, and hydrofluoric acids using hydrothermal treatment. Hydrofluoric acid treated TiO_2 support samples were found to be the most effective additive with spherical shapes and the catalysts were more uniformly dispersed with a smaller particle size compared to other samples.

TiO_2 nanofiber mat was developed and as-synthesized mat was immersed in the mixture of ethylene glycol, H_2PtCl_6, and polyvinyl pyrrolidone (PVP) which results in the deposition of Pt nanoparticles on to TiO_2 nanofibers. Formo et al. [52] found that the Pt nanoparticle density increased proportionally with the duration and this deposited Pt act as seeds which leads to the formation of nanowires. Titania supported nonprecious metals (polyaniline (PANI)-treated TiO_2 nanoparticles with Fe nanoparticles) also have been investigated to improve the electrocatalytic performance [53] of ORR. In order to explore the roles of TiO_2, iron, and nitrogen from PANI, the ORR performance of the prepared electrocatalyst was compared with PANI−Fe supported on commercial carbon black. The authors claimed that the ORR activity is due to increase of electronic conductivity and the presence of anatase phase. The 40 wt.% Pt supported on graphene/TiO_2 composite electrocatalyst have been studied for ORR. In which the polyol method was used to deposit Pt on titanium dioxide functionalized graphene nanosheets and the ORR were evaluated in both acidic and alkaline medium. Though it follows four electron reduction of oxygen to H_2O, the accelerated durability test results showed slightly lower stability as compared to Pt/C [54]. Similarly, TiO_2 nanofibers wrapped with rGO (h-rGO@TiO_2−rGO) was synthesized using hydrothermal method followed by the Pt nanoparticle deposited using polyol method. Fig. 26.3 shows the synthesis scheme of the electrocatalyst and their cyclic voltammetry (CV) result showed the ECSA value of 30.95 m^2/g [55].

Huang et al. [50] studied the cathode catalytic performance of Pt/Pd supported on TiO_2. Their observation revealed that the catalytic activity has been increased with 30% of bimetallic alloy and beyond that composition, the activity was found to be reducing due to the blocking of Pt active sites by a large amount of Pd. Their halve cell study demonstrated that Pt70Pd30 had similar activity of Pt/C (TKK) and fourfold increase in ORR activity. Interestingly, Huang et al. produced Pt supported TiO_2 thin films on fluorine−doped tin oxide glass by screen printing method. Further they claimed that the synergetic effect of mesoporous thin film and stronger interaction of Pt−TiO_2 promoted the higher activity and stability of ORR in acidic medium [56]. Xu et al. [57] enhanced the ORR activity of $Ru_{85}Se_{15}$/C electrocatalyst by modifying them with TiO_2. Their results showed higher electrochemical stability in $Ru_{85}Se_{15}$/TiO_2/C. The initial activity of $Ru_{85}Se_{15}$/TiO_2/C is similar to $Ru_{85}Se_{15}$/C, but final potential of $Ru_{85}Se_{15}$/TiO_2/C is higher than the potential of $Ru_{85}Se_{15}$/C. Fig. 26.4 shows the stable single-cell testing performance of $Ru_{85}Se_{15}$/TiO_2/C compared to $Ru_{85}Se_{15}$/C. They found that TiO_2 prevented $Ru_{85}Se_{15}$ nanoparticle aggregation due to the effects such as anchoring, steric hindrance, and stabilization of Se, which is considered as an excellent antioxidant for Ru.

Chevallier et al. proposed a highly active and stable Pt/5%Nb−TiO_2 carbon-free cathode electrocatalyst for PEMFC. Similarly, Wu and Yang established a two-step approach of electrospinning and atomic layer deposition method for the synthesis of Pt@Nb−TiO_2 nanofiber-based electrocatalyst for ORR. Fig. 26.5 shows the two-step preparation method scheme of atomic layer

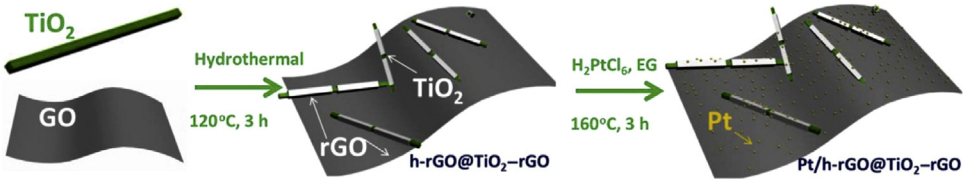

FIGURE 26.3 A schematic of the preparation method of Pt/h-rGO@TiO_2 hybrid electrocatalyst. *rGO*, reduced graphene oxide; *TiO_2*, titanium oxide or titania. *Reprinted from W. Zhuang, L. He, J. Zhu, R. An, X. Wu, L. Mu, et al., TiO2 nanofibers heterogeneously wrapped with reduced graphene oxide as efficient Pt electrocatalyst supports for methanol oxidation, Int. J. Hydrogen Energy 40 (2015) 3679−3688. Available from: https://doi.org/10.1016/j.ijhydene.2015.01.042* ©2015 Elsevier.

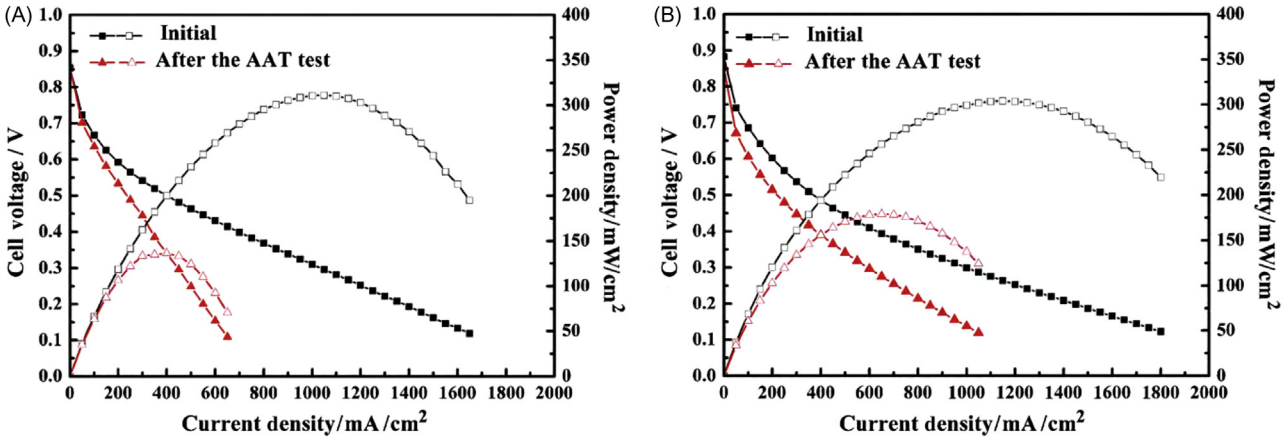

FIGURE 26.4 Cell performances of (A) $Ru_{85}Se_{15}$/C MEA and (B) $Ru_{85}Se_{15}/TiO_2$/C MEA before and after the acceleration durability test for 1000 cycles between 0.6 and 1.0 V vs reversible hydrogen electrode (RHE). *MEA*, membrane electrode assembly; *TiO_2*, titanium oxide or titania. *Reprinted from T. Xu, H. Zhang, H. Zhong, Y. Ma, H. Jin, Y. Zhang, Improved stability of TiO2 modified Ru85Se15/C electrocatalyst for proton exchange membrane fuel cells, J. of Power Sources 195 (2010) 8075–8079. Available from: https://doi.org/10.1016/j.jpowsour.2010.07.019. ©2015 Elsevier.*

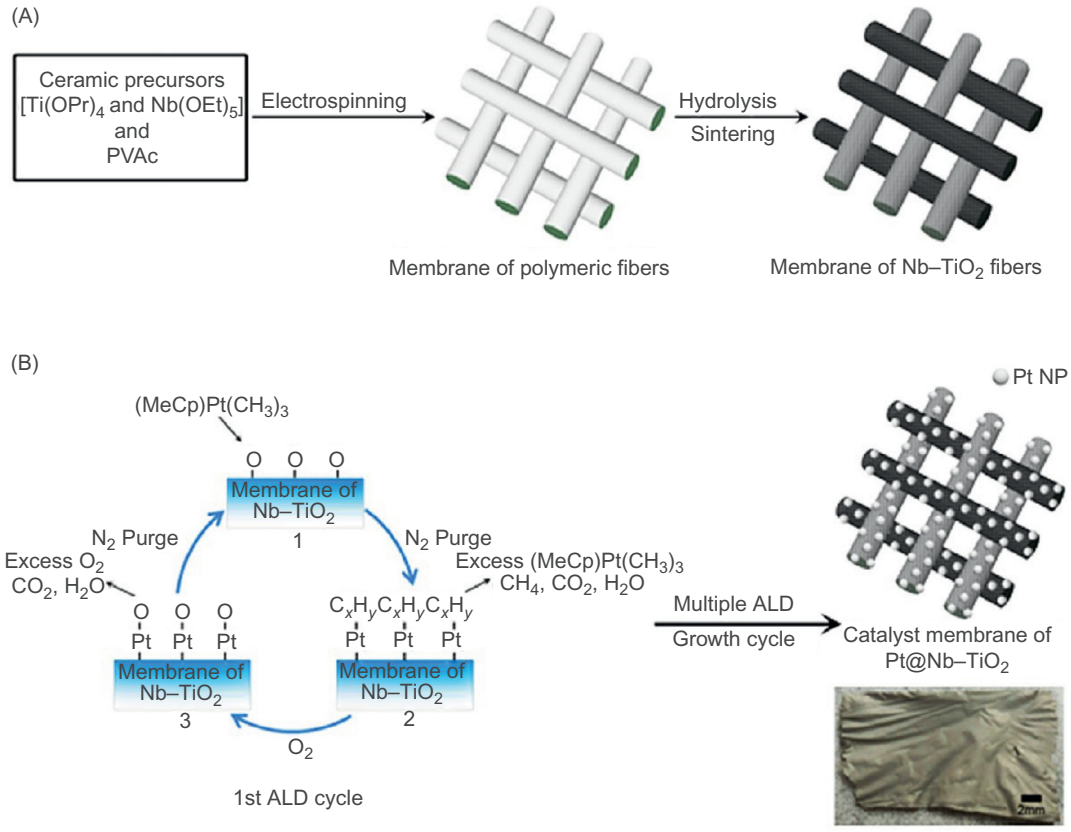

FIGURE 26.5 Schematic illustration of the preparation process of Pt@Nb−TiO_2 catalyst membrane: (A) preparation of Nb−TiO_2 fiber-woven membrane by electrospinning technique and pyrolysis; and (B) deposition of Pt nanoparticles onto Nb−TiO_2 by atomic layer deposition technique. *TiO_2*, titanium oxide or titania. *Reprinted from Q. Du, J. Wu, H. Yang, Pt@Nb_TiO2 catalyst membranes fabricated by electrospinning and atomic layer deposition, ACS Catal. 4 (2014) 144–151. Available from: https://doi.org/10.1021/cs400944p. ©2014 American Chemical Society.*

deposition of Pt on electrospun Nb−TiO_2 nanofibers [58]. The area-specific ORR activity of the Pt@Nb−TiO_2 was 0.28 mA/cm^2_{Pt} at 0.9 V and accelerated-stability test showed that it has very high stability [59].

Akalework et al. [60] reported the preparation of TiO_2-coated MWCNTs support material with an excellent electrical conductivity for improving the kinetics of ORR. The Pt-based MWCNT@TiO_2 electrocatalyst was showing an

ECSA of 285.5 m^2/g, which is comparatively higher than Pt/MWCNT (188.2 m^2/g) and Pt/C (153.4 m^2/g) and the ORR polarization results of Pt−MWCNT@TiO_2 displayed more positive onset potential.

26.8 TITANIUM DIBORIDE

A highly stable, electrically conducting and corrosion resistant ceramic TiB_2 has also been used as support material for Pt catalyst PEMFC. TiB_2 is a ceramic material that has good electrical conductivity, corrosion resistance and thermal stability in acidic medium [61]. For the first time in 2010, Yin et al. [62] showed an electrochemical stability of TiB_2 supports which is four times higher than commercial Pt/C. In contrast, the same authors also prepared Pt/TiB_2 electrocatalyst from Nafion stabilized Pt nanoparticles (Fig. 26.6) and extensively studied the performance of PEMFCs. The performance obtained was comparatively similar to their next work [63].

In 2011, Yin et al. supported the Pt electrocatalyst on surface-stabilized TiB_2 with Nafion for more stable performance. The schematic diagram of the electrocatalyst preparation method is shown in Fig. 26.7. Though the initial ECSA of Pt/TiB_2 (37.5 m^2/g) is lower than a commercial 20 wt.% Pt/C catalyst (61.4 m^2/g), the ORR results showed higher reduction current of 0.3 mA/cm^2 at 0.9 V for Pt/TiB_2 as compared to 0.12 mA/cm^2 at 0.9 V.

Huang et al. [64] investigated the effect of pretreated TiB_2 with HCl, H_2O_2, ammonia, and NaOH for the use of catalyst support in fuel cell applications. Their CV and polarization curves indicated that the H_2O_2 pretreated showed higher ECSA (26.7 m^2/g) and current density (0.77 mA/cm^2) as compared to other materials.

26.9 TITANIUM NITRIDE

Another well studied Ti-based material is TiN and this triple bond transition metal compound is corrosion resistant and it has high electrical conductivity (4000 S/m) and high mechanical hardness [65,65a,66]. These excellent properties of TiN make it a more suitable electrocatalyst support material for PEM fuel cells. For example, Musthafa and Sampath developed a well dispersed Pt on TiN as an electrocatalyst support system [67] and Avasarala and Halder [68] reported the preparation of Pt/TiN using commercial TiN nanoparticles as an anode catalyst support for PEMFCs. Though the results are comparatively higher than commercial Pt/C catalyst, it suffered in terms of long-term stability in acidic medium. Recently, the same group studied the durability and stability of TiN nanoparticles under fuel cell conditions. They supported Pt nanoparticles on commercial TiN nanoparticles (particle size of 20 nm and specific area of 40−55 m^2/g) using the polyol process. Their study was carried out in sulfuric acid electrolyte at various operating temperatures and results showed that an active behavior of Pt/TiN was observed for optimal conditions of 0.5 M H_2SO_4 and at 60°C. Pan et al. [69] described the synthesis route for the development of TiN nanotubes-based

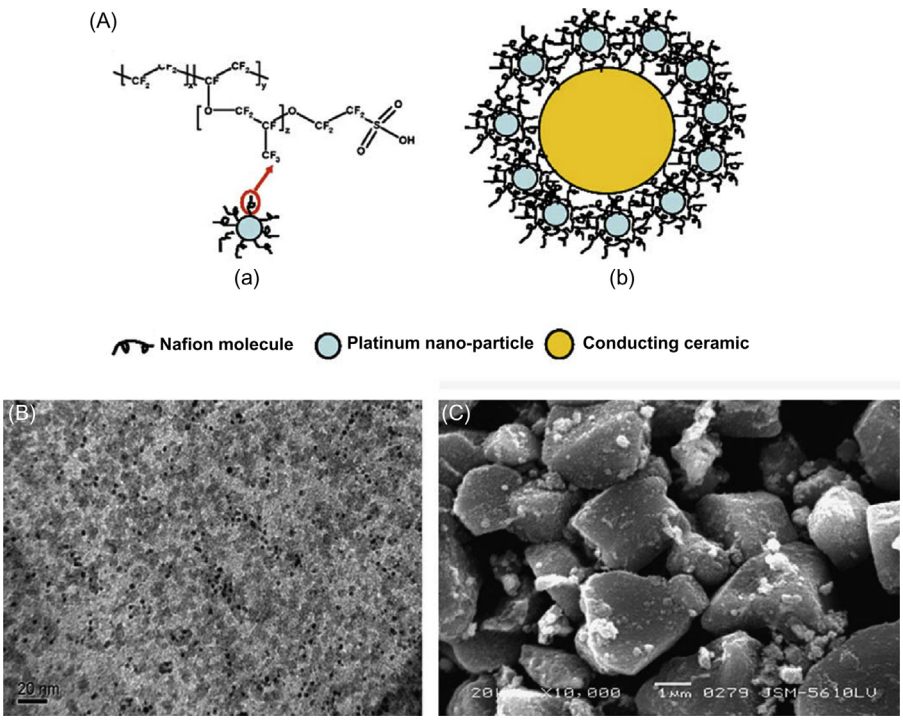

FIGURE 26.6 A schematic of the Pt/TiB_2 catalysts with perfluorosulfonic acid Nafion as a stabilizer of Pt particles (A), transmission electron microscopy (TEM) image of the Pt colloid particles (B), and scanning electron microscopy micrograph of TiB_2 powders (C). *Reprinted from S. Yin, S. Mu, H. Lv, N. Cheng, M. Pan, Z. Fu, A highly stable catalyst for PEM fuel cell based on durable titanium diboride support and polymer stabilization, Appl. Catal., B 93 (2010) 233−240. Available from: https://doi.org/10.1016/j.apcatb.2009.09.034.* ©2010 Elsevier.

support material for Pt electrocatalyst. Their accelerated durability test (ADT) showed higher stability and also showed minimum ECSA loss compared to commercial catalyst. They claimed that the performance and stability was mainly due to the hollow structure and porous walls and strong interaction between Pt and TiN nanotubes support. Similarly [70], also demonstrated the electrochemical activity and durability of Pt-supported TiN electrocatalyst toward ORR. They obtained the mass activity of 0.29 A/mg for 10 wt.% Pt/TiN and their polarization curve displayed only 6.2 mV difference of half wave potential (Fig. 26.8), whereas Pt/C showed 24.2 mV which suggested that TiN-based electrocatalyst was more durable for ORR.

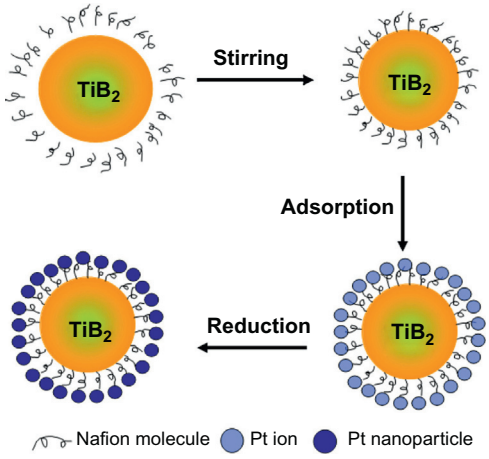

FIGURE 26.7 A schematic illustration of the preparation method of Pt/TiB_2 catalysts. *Reprinted from S. Yin, S. Mu, M. Pan, Z. Fu, A highly stable TiB2-supported Pt catalyst for polymer electrolyte membrane fuel cells, J. Power Sources 196 (2011) 7931–7936. Available from: https://doi.org/10.1016/j.jpowsour.2011.05.033. ©2011 Elsevier.*

Jiang et al. [106] attempted to replace precious noble metals by preparing a hybrid of TiN and nitrogen doped carbon on SiC for PEMFCs reaction. The claimed that the activity and durability was mainly attributed because of the synergetic effect of TiN and nitrogen doped carbon [71]. studied the effect of shape specific electrocatalytic activity by changing the morphology of TiN catalysts from nanoparticle to nanotubes and they showed remarkable performance. Surprisingly, Kim et al. [72,73] reported the preparation Pt supported TiN nanofibers using electrospinning method for PEMFCs electrodes. The synthesis process and their X-ray powder diffraction results of TiN nanofibers is shown in Fig. 26.18. Their durability results (Fig. 26.9) obtained from polarization and CV curves suggested that the TiN nanofibers-based electrocatalyst was more stable as compared to commercial Pt/C.

26.10 TUNGSTEN OXIDE

Tungsten is an adaptable element which can possibly form various oxides (oxidation states from −1 to +6) and carbides. Tungsten oxide is an n-type semiconducting material with a band cap of 2.6–2.8 eV. Particularly, Pt or Pt alloy supported on tungsten oxide-based electrocatalysts give good performance and more resistance to corrosion. The most stable state is hexavalent tungsten oxide, WO_3, which has poor electronic conductivity due to its large bandgap [74,75]. The intrinsic electric conductivity of tungsten oxide arises from its nonstoichiometric composition, oxygen-vacancy defects in the lattice formed donor level [76]. A detailed review on tungsten-based support materials in various aspects of fuel cells have published by [77]. Even though a variety of synthesis routes such as sol–gel [78,79], coelectrodeposition [80],

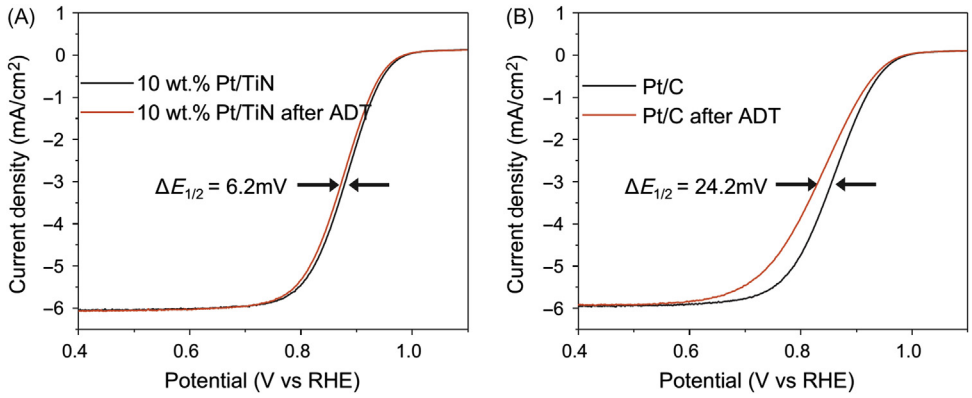

FIGURE 26.8 ORR polarization curves before and after ADT for (A) 10 wt.% Pt/TiN catalyst and (B) 20 wt.% Pt/C catalyst in O_2-saturated 0.1 M $HClO_4$ with a scan rate of 10 mV/s and a rotation rate of 1600 rpm. *ORR*, oxygen reduction reaction; *ADT*, accelerated durability test. *Reprinted from S. Yang, D. Young, Y. Tak, J. Kim, H. Han, J. Yu, et al., Electronic structure modification of platinum on titanium nitride resulting in enhanced catalytic activity and durability for oxygen reduction and formic acid oxidation, Appl. Catal., B 174–175 (2015) 35–42. Available from: https://doi.org/10.1016/j.apcatb.2015.02.033. ©2015 Elsevier.*

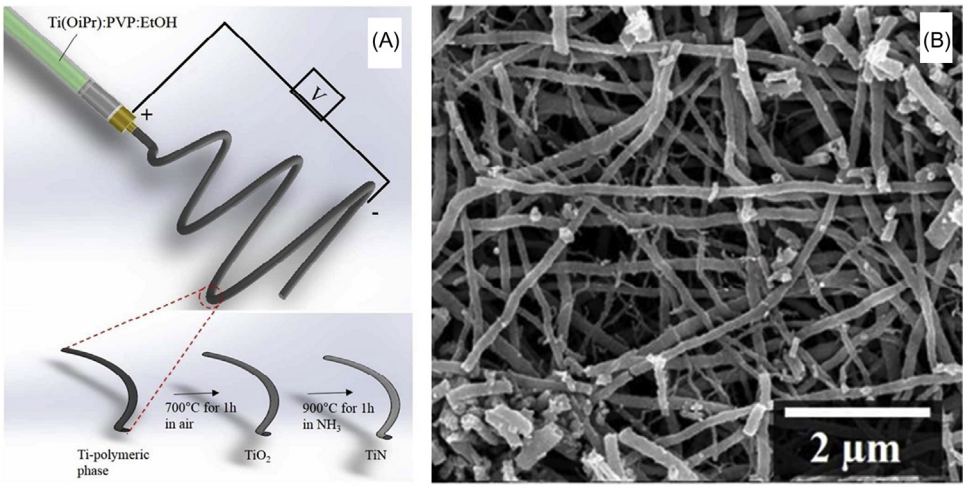

FIGURE 26.9 Schematic illustration of TiN nanofiber synthesis route and scanning electron microscopy images of the prepared TiN nanofibers. *Reprinted from J. Kim, Y.-S. Chun, S.-K. Lee, D.-S. Lim, Improved electrode durability using a boron-doped diamond catalyst support for proton exchange membrane fuel cells, RSC Adv. 5 (2015) 1103–1108. Available from: https://doi.org/10.1039/C4RA13389G; H. Kim, M.K. Cho, J.A. Kwon, Y.H. Jeong, K.J. Lee, N.Y. Kim, et al., Highly efficient and durable TiN nanofiber electrocatalyst supports, Nanoscale 7 (2015) 18429–18434. Available from: https://doi.org/10.1039/C5NR04082E.* ©*2015 Royal Society of Chemistry.*

cosputtering [81], and freeze–drying [82] have been adopted for the Pt/WO_x, sol–gel method gives numerous benefits including higher surface area, easy synthesis, and smaller particle size. Various morphologies of tungsten oxide like microsphere and nanorods have also been studied as catalyst support for PEMFCs and direct methanol fuel cells [37,83]. Although a Pt-based tungsten oxide electrocatalysts exhibits higher stability [98], tungsten dissolution is still observed [84]. The WO_3 chemical instability in acidic medium is still persisting as the major issue that restricts its application in fuel cells. There have been lot of efforts made to improve the suitably by adjusting the conditions of its preparation, for instance the incorporation of Ti^{4+} with a minimum concentration in the WO_3 framework, enhances the stability of WO_3. This, further, decreases its ohmic resistance with the increase in the Ti^{4+} substitution in the WO_3 framework [14]. Carbon-coated tungsten oxide nanowires as a cathode electrocatalyst support material was prepared by [85]. The nanowires were directly grown on carbon paper using CVD process and the Pt nanocatalyst was deposited using glacial acetic acid as the reducing agent. An electrochemical study revealed that the as-prepared support material had higher mass specific surface area compared to commercial Pt/C electrode. In addition to that, +100-mV potential shift was also observed in the onset potential for the ORR and also displayed 75% higher mass activity and higher ORR current than that of commercial Pt/C. In order to study the effects of tungsten oxide supports in the electrodes, different thickness level of WO_x (0–40 nm) were prepared with and without Pt (3 nm) electrocatalysts using thermal evaporation method (Fig. 26.10). The anode reaction (HOR) has been performed with and without spraying of Nafion onto the electrodes. The measurement showed that the higher surface area of Pt on thicker tungsten oxide thin films was suggested for the benefit of limiting current in the HOR. Moreover, a less ECSA was observed in the electrode without Nafion content [86]. Hengge et al. [37] described the two-step template-free approach for growing highly porous networks of Pt nanorods on WO_{3-x}. Their study revealed that the overall ECSA was increased with the longer time of reduction process. Liu et al. [78] prepared nanosized tungsten oxide crystals followed by the Pt deposited via galvanic displacement of a Cu layer by Pt using electrochemical method. In which the working electrode was initially covered with Cu monolayer by underpotential deposition and further placed into aqueous solution of K_2PtCl_4 and H_2SO_4 for 4 minutes to replace Cu with monolayer Pt particles. They clearly showed the degradation mechanism of WO_3 and the detachment of Pt nanoparticles and also suggested the alternative structures, such as Pt–WC or Pt–WO_3 core shell structures, for the improvement of ORR activity.

26.11 TUNGSTEN CARBIDE

Tungsten carbide is well known for its hardness, good electrical conductivity (105 S/cm for WC at 20°C), and it is resistant to chemical attack. However, it undergoes surface oxidation and dissolution when it is exposed to air and water. The Fermi level of tungsten carbide is near and the electronic state of tungsten carbide is similar to those of platinum metal, in its noble form [87,88]. Because of these similar properties, tungsten carbide has received more attention as catalyst supports, co-catalysts, as well as electrocatalysts [59,83,89]. Generally, most important tungsten carbide phases are tungsten monocarbide (WC) and tungsten subcarbide (W_2C). W_2C is thermodynamically unstable at lower temperatures below 900 °C when compared to WC [90]. Tungsten carbides also enhanced ORR at the cathode [91]. Most commonly

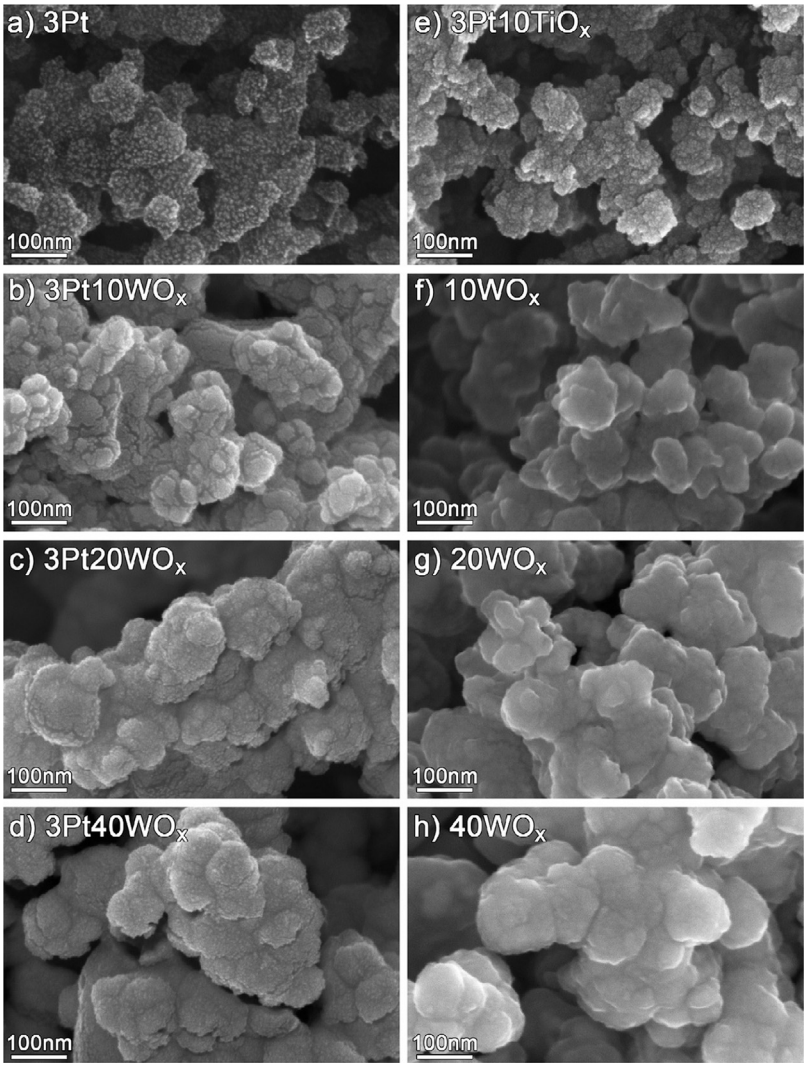

FIGURE 26.10 Scanning electron microscopy images of the as-prepared Pt/WO_x thin film model electrodes deposited on GDL. *GDL*, gas diffusion layer. *Reprinted from B. Wickman, M. Wesselmark, C. Lagergren, G. Lindbergh, Tungsten oxide in polymer electrolyte fuel cell electrodes—a thin-film model electrode study, Electrochim. Acta 56 (2011) 9496–9503. Available from: https://doi.org/10.1016/j.electacta.2011.08.046. ©2011 Elsevier.*

used tungsten carbides are WC and W_2C. The study conducted by [92] shows that WC remained stable at an anode potential of 0.6 V in 0.5 M H_2SO_4. Different pore size of three-dimensionally ordered macroporous tungsten carbide was prepared by Bosco et al. adopting the "inverse-opal" method [89]. Zhou et al. [93] also prepared Pt nanoparticle supported on mesoporous tungsten carbide by coassembly followed by sodium borohydride reduction method. Interestingly, the WC nanofibers structure with Pt nanoparticles were prepared by electrospinning followed by pyrolysis process using ammonium metatungstate and PVP as precursor materials. The ORR performance and kinetic results revealed that it follows more stable performance and four electron pathways in alkaline solution (KOH). However, achieving optimal Pt particle size and dispersion on these carbide structures are still a challenging task, which need to be addressed. Nie et al. [94] also demonstrated the catalytic activity of the Pt–WC/C electrode for ORR which is higher than that of Pt/C and they claimed that it is due to the synergistic effect between Pt and WC. These results indicate that tungsten carbides are promising for catalyst supports. Some other studies were also carried out on Pt–Ru alloy catalysts supported on tungsten carbide to show the suitability [95,96]. Moreover [97], also made a comparison between Pt/WC and Pt/C, suggesting that Pt/WC possessed a higher stability and cell performance in a fuel cell environment, while the effective catalytic surface area was lower than that of Pt/C. Even though it has more benefits on catalytic activity and durability, but still there are some challenges in carbides as it appears too poor to be used as catalyst support material. For instance, the ECSA of Pt/WC is considerably low, which indicates that the controlling of particle size is very important [98,99]. Hence, controlling the size and dispersion of the electrocatalyst on WC needs to be thoroughly investigated to attain the feasible performance. Pt and Pt–Ru alloy catalyst supported on WC were studied as electrocatalysts for

PEMFCs by Lust et al. The micromesoporous texture with high surface area (2116 m^2/g) of WC showed the current density of 150 A/m^2 with four-electron pathway mechanism. Surprisingly, a novel route was adopted by [100] to develop nanosized tungsten carbide using ion exchange mechanism with Pt as an electrocatalyst and their results displayed an electrochemical mass activity of 257 mA/mg_{Pt} at 0.9 V. Han et al. [101] reported the preparation of tungsten carbide and CNT−graphene (CNT−GR) supported Pd electrocatalyst for HOR. It was found that Pd/WC/CNT−GR electrocatalyst showed high ECSA (36.3 m^2/g) and maximum power density (464 mW/cm^2) compared to other prepared Pd-based WC catalysts. Similarly, the composites of WC also modified with materials, such as carbon black, MWCNTs, hybrid ordered mesoporous carbon (OMC), hollow microspheres, nitrogen-doped carbon and PANI coating for improving the performance and durability [102−106].

26.12 TIN OXIDE

SnO_2 is a transition metal dioxide with rutile structure and is normally considered as an oxygen deficient n-type semiconductor. The profound chemical properties include the adsorption of OH species at low potentials and ability to induce electronic effect with Pt has accelerated to perform SnO_2 as a challenging fuel cell electrocatalyst support [77]. The Sun et al. group demonstrated the directly grown SnO_2 nanowires on carbon paper with an electrochemically deposited Pt and Pt alloy (PtRu) nanoparticles as the fuel cell support material. The SnO_2 nanowire-based electrode showed an enhanced electrocatalytic activity toward fuel cell reactions as compared with commercial Pt/C (30 wt.% ETek) [107]. Similarly, Zhang et al. [108] prepared mesoporous SnO_2 with high surface area (205 m^2/g) and oxidation resistant support material using neutral surfactant template-assisted method and the Pt nanocatalyst was distributed using modified polyol process. They studied and compared the performance and stability of Pt/SnO_2 system with commercial Pt/C (Vulcan XC-71 and Ketjen Black EC 300J). Their comparative results showed similar electrochemical activity and notably enhanced electrochemical stability in Pt/SnO_2 especially at high potential. Furthermore, tin oxide-based support materials are also expected to get the better durability. The Nakkada and their group predicted that SnO_2 mainly influenced the oxidation and reduction behavior of supported Pt. The authors claimed that this is due to the strong interaction of SnO_2 and Pt, which makes the Pt more durable. Surprisingly, the author found its instability due to the redox properties under electrochemical conditions [109]. SnO_2 nanowire-based structures also have been tried with electrochemically deposited Pt [107]. The SnO_2 nanowires were directly grown on the carbon fibers of carbon paper using thermal evaporation method with an electrochemical deposition of Pt and the results showed comparatively improved ECSA for Pt/SnO_2 nanowire-based electrode (54.7 m^2/g) over commercial Pt/C (E-TEK) (33.6 m^2/g) in acidic medium. The ORR results showed a positive shift (50 mV) in the onset potential and reduction peak current of 13.3 mA/mg_{Pt} which is 1.6 larger than Pt/C electrode. Surprisingly Cavaliere et al. reported the preparation of antimony-doped SnO_2 loose tubes using an electrospinning method for the catalyst support material of PEMFCs electrodes. In this, the polyol method was adopted to deposit Pt nanoparticles with an optimal dopant (Sb) concentration of SnO tubes. They found Pt/SnO_2 tubes showed higher ORR mass activity and stability as compared to commercial Pt/C [110]. Similarly, they also prepared niobium-doped SnO_2 tubes from an electrospinning method and obtained the highest electrical conductivity of 0.02 S/cm. Further, they suggested the use of support material due to its unique properties, such as surface area, electrochemical conductivity, and electrochemical stability at high potential [111]. Niobium- and antimony-doped SnO_2 aerogels have been prepared to improve the electrical conductivity (1 S/cm) which is nearer to Vulcan XC-72 (4 S/cm), and they claimed that the high surface area (60 m^2/g) with mesoporosity can form the uniform dispersion of catalyst for the possible use of electrodes in fuel cells [112]. Pt−SnO_2 with nitrogen-doped CNT hybrid electrocatalyst also have been tested as support material for the stable performance of PEMFCs [113]. The detailed study performed by [38] on SnO_2-mesoporous carbon (CMK-3) composite with platinum support material showed the ORR current density of 3.40 mA/cm^2 at an electrode potential of 0.9 V vs RHE and it followed predominantly the four-electron pathway. Moreover, ITO also has got significant attention over the past few decades as a electrocatalyst support material for PEMFCs. Chhina et al. recently studied the potential of ITO toward oxidation-resistant catalyst supports in PEM fuel cells. Even though, it is showing more resistance to oxidation compared to Vulcan XC-72R, the catalytic activity is not found toward ORR [40]. Chang et al. analyzed the electrocatalytic properties of Pt nanoparticles supported on ITO and Pd nanoparticles supported on ITO for PEMFCs reaction. The oxygen reduction performance of both electrocatalysts was shown to be similar to that of bulk Pt and Pd, respectively. These reveal that ITO can be a promising support for fuel cell catalysts [114,115].

26.13 SILICON DIOXIDE

Silicon dioxide or silica is generally known for its hardness and exists in both amorphous and various crystalline forms. Generally the silica was used in fuel cells for the

preparation of self-humidifying membranes. Very recently, Seger et al. [39] studied silica as a support material for the cathode electrocatalyst. Sodium borohydride was used as a reducing agent to prepare Pt nanoparticles on a colloidal silica substrate. They found that the lower concentrations of Pt produced uniform Pt dispersions (4 nm) with interconnected particle-network enabling higher conductivity and higher surface area. The authors compared the performance of as-prepared core-shell Pt/SiO_2 with commercial E-TEK. The results showed higher electrocatalytic active area, and improved charge transfer kinetics for Pt−SiO_2. Interestingly, the carbon nitride-modified SiO_2 support material with Pt electrocatalyst was prepared by [116] for ORR. The composite support was prepared via in situ polymerization using calcinations of polypyrrole (PPy)-coated SiO_2 and the Pt nanoparticles were dispersed using polyol process. The report displayed that as-prepared support material showed an ECSA of 89.6 m^2/g which is comparatively higher than Pt/C and also exhibited much higher durability. They claimed that the improved activity, durability, and performance of the composite support was due to the synergetic effect of oxophilic behavior of SiO_2, N species, and the strong interaction of catalyst and the support.

26.14 CARBON-BASED SUPPORT MATERIALS

Various carbon materials, such as Vulcan XC-72R [117], MWCNT [118−120], graphite nanofibers [119], activated carbon [21,22,121,122], carbon black, and graphite [121], are being extensively used as support materials for Pt nanocatalyst particles for PEM fuel cells. In recent years, metal-free electrocatalysts in the form of mono, binary, or ternary N-, S-, B-, and P-doped carbon nanomaterials, such as graphene, CNTs, CNFs, have been introduced for enhanced catalytic activity for fuel cell reactions due to the conjugation between the π electrons of carbon and the lone pair electrons from dopants [33,123,124]. These metal-free electrocatalytic materials have gained great attention in fuel cell reactions because of their unique properties, such as high activity, low price, and high stability [125−127].

26.15 CARBON BLACK

Generally, when the carbon containing materials undergo heat treatment processing under inert or oxygen-free environment they are called carbon black. The spherical-shaped amorphous carbon usually will be below 50 nm in size. The particles can agglomerate and the size can vary up to 250 nm. The carbon black particles are constituted by individual building blocks of graphitic layer and each crystallite are turbostratic layers having an interlayer spacing of 0.35−0.38 nm. The applicability of Pt-supported carbon black as an electrocatalyst has attracted researchers' attention due to its easy availability, low cost, high surface area, and good electrical conductivity. Commercial electrocatalysts for PEMFCs include Cabot Corporation (Vulcan XC-72R, Black Pearls BP 2000), Chevron (Shawinigan), Ketjen Black International, Denka, and Erachem [128]. The most extensively used carbon blacks (especially Vulcan XC-72) are usually supported with Pt or Pt-alloy catalysts for fuel cells. Interestingly, Ag nanoparticles decorated with Pt were synthesized by [129] for ORR. The Pt/Ag bimetallic mixed alloy catalyst supported on carbon black was prepared by thermal treatment at 300°C. Dodelet et al. [130] prepared Pt nanowires (PtNWs) on CB supports using the mixture of chloroplatinic acid and formic acid with different amounts of Vulcan XC-72. The results suggested that the mass ratio between carbon and the Pt precursor and decreasing the time duration are the factors for controlling the growth density and the length of the nanowires. They also observed that 50% PtNWs loaded on carbon black displayed greater activity compared to commercial catalysts which is due to the specific crystallography of PtNWs and the presence of surface defects. Electrocatalysts of Pt supported on nitrogen-doped carbon black (Pt/NCB) was prepared by Zhang and Chen [131]. They found an increased dispersion of Pt nanoparticles on NCB compared to that on pristine CB which exhibited high surface area and specific activity for ORR [132]. Recently, Bae et al. [133] also developed NCB electrocatalyst from acetonitrile pyrolysis for HOR. In order to improve the stability of the support material [134], made an attempt to produce hybrid support material of zirconia−carbon for Pt catalysts. Their accelerated durability tests revealed that ZrO_2−C composites displayed more stability compared to Pt/C. Interestingly, Kakaei reported the preparation of Pt/Vulcan carbon-PANI (Pt/VC-PANI) fiber for cathode electrocatalyst of PEMFCs. The performance of Pt/VC-PANI was found to be 1.82 and 1.3 times higher than commercial Pt/C (E-TEK) and Pt/C (E-TEK) + PANI catalyst (Fig. 26.2) [135]. Similarly, Memioğlu also investigated the electrochemical stability of PPy/carbon composites based support material for PEMFC applications [136]. Senthil Kumar et al. pretreated Vulcan XC-72 with HNO_3, H_3PO_4, KOH, and H_2O_2 to change the surface chemical properties and surface area. They found that the surface area and pore volume of 5% HNO_3 and 10% H_2O_2 treated samples were drastically reduced due to their oxidative nature. On the other hand, treatment with 0.2-M KOH and 0.2-M H_3PO_4 removed 50% of sulfur Vulcan XC-72 support without altering the surface area and micropore volume [137]. However, carbon black generally suffers major problems, such as deep micropores (which trap the catalyst and are

further inaccessible to reactants), presence of organosulfur impurities, carbon corrosion, Ostwald ripening, and Pt dissolution, which lower the activity and durability of the electrocatalysts during long operations [138]. These smaller pore sizes also affect the interactions between catalyst and ionomer particles (Nafion micelles >40 nm) which leads to no contribution in electrochemical activity. Elaborate studies on novel electrocatalysts, such as CNFs, mesoporous carbon, CNTs, graphene, have been discussed in the following sections. The unique property of each material provides high ECSA, improved catalyst efficiency, and better durability. Hence, these properties are extremely desirable for reducing catalyst loadings and thereby greatly lower the overall cost of the fuel cells.

26.16 CARBON NANOTUBES

During the past few decades, both single-walled CNTs (SWCNTs) and MWCNTs have been broadly explored for the application of support material in PEMFCs. The pristine CNTs are chemically inert and the functionalization with harsh acidic treatments (HNO_3, H_2SO_4, $K_2Cr_2O_7$, H_2O_2, etc.) or electrochemical reactions are needed to introduce functional groups [carboxyl (−COOH), hydroxyl (−OH), or carbonyl (−C = O)] on the surface for improving the catalyst support interactions [139,140]. Another important functionalization of CNTs to uniformly disperse nanoparticles is based on ultrasound treatment. Based on this [141], demonstrated the role of ultrasonic, sonochemical, and sonoelectrochemical methods for the preparation of carbon support with catalysts of mono- and bimetallic nanoparticles for fuel cell electrodes. The surface modified CNTs have been employed as the support for monometallic, bimetallic (Pt−Ru, Pt−Ag, Pt−Co, Pt−Fe, etc.), and even for trimetallic (Pt−Ru−Pd, Pt−Ru−Ni, Pt−Ru−Os, etc.) catalysts. Interestingly, Du et al. [142] fabricated mesoporous SnO_2-coated CNT by a hydrothermal method as a stable support material for Pt catalyst. At high potentials, the anodic current of CNT@SnO_2 core sheath nanocomposites are much lower than CNT support catalyst (Pt/CNT) and also are more durable. Uniformly dispersed Pt catalyst on SWNTs and C nanocomposites electrocatalysts was prepared by [143] for PEMFC. The performance was evaluated with different weight percentage of Pt/CNT and Pt/C which indicated that 50:50 gives better performance. SWCNTs and platinum were used as support material and catalyst, respectively. By means of electrophoretic deposition method, Pt and SWCNTs were cast on a carbon fiber electrode (CFE). Lower charge-transfer reaction resistance was observed than that of commercial carbon black-based electrodes. Fuel cell testing results of CFE/SWCNT/Pt-based electrodes showed higher maximum power density than the conventional electrodes [144]. Tang et al. [145] prepared Pt nanodots (2−3 nm) supported on CNTs as an electrocatalyst on carbon paper by employing sputter deposition and in situ reduction method. The combined system of GDL and catalyst layer demonstrated maximum power density of 595 mW/cm^2 for a catalyst loading of 0.04 mg/cm^2. This result showed significantly higher performance compared to commercial electrocatalysts, e.g., Pt supported on Vulcan XC 72R-based electrode (435 mW/cm^2 for same loading of catalyst). Shen et al. [146] attempted to reduce the catalyst loading in electrodes of PEMFCs by developing the vertically aligned CNTs grown on Al foil as the catalyst support material using plasma-enhanced chemical vapor deposition method. Their results indicated that the maximum power density 697 mW/cm^2 was achieved with Pt loadings of 108 μg/cm^2 at anode and 102 μg/cm^2 at cathode, which is 21% higher compared to that of the commercial catalyst. Moreover, the introduction of conjugated polymers such as PANI and PPy forming covalent bonds between Pt atoms and N atoms makes strong linkage of Pt nanoparticles with PANI [147−149]. Based on this concept, He et al. [150] prepared Pt nanoparticles on MWCNTs wrapped with PANI which demonstrated that PANI acted as a bridging component between Pt nanoparticles and MWCNTs (Fig. 26.11) and also revealed that Pt/MWCNT functionalized with PANI showed an improved electrocatalytic activity and better stability as compared to carbon black support.

Chen et al. [151] studied the effect of nitrogen doping on CNTs for improving the activity of ORR. The Pt loaded on nitrogen-doped CNTs displayed higher ECSA, current density, and power density of 41.8 m^2/g, 0.230 A/cm^2, and 0.87 W/cm^2, respectively, whereas Pt/CNTs showed only 26.1 m^2/g, 0.144 A/cm^2, and 0.47 W/cm^2. Similarly, the composite nanostructure-based support materials of nitrogen-doped CNTs coated with $TiSi_2O_x$ was synthesized using the combination of chemical vapor deposition and magnetron sputtering method for ORR in PEMFCs. They found that $TiSi_2O_x$ formed an amorphous layer with different thickness on CNTs and the electrocatalytic properties of Pt supported on $TiSi_2O_x$-NCNTs showed a positive potential of 30 mV, higher mass, and specific activity toward ORR [152]. Surprisingly, Long et al. [153] prepared Pt-supported partially unzipped CNTs as the catalyst support material for PEMFCs. The CNTs were partially unzipped using strong oxidation with $KMnO_4$ and rapid heat expansion (Fig. 26.12). The prepared material showed high specific area 168 m^2/g compared to parent CNTs (72 m^2/g) which led to an increase in the accessibility of outer and inner walls of CNTs. The electrochemical performance of the Pt loaded on partially unzipped CNTs showed higher ECSA of 129 m^2/g as compared to Pt/CNTs (64 m^2/g) and Pt/Vulcan (71 m^2/g). The electron transfer number of ORR was 3.6 which indicated the complete reduction of O_2 into H_2O through the four-electron pathway. Recently, cobalt and its

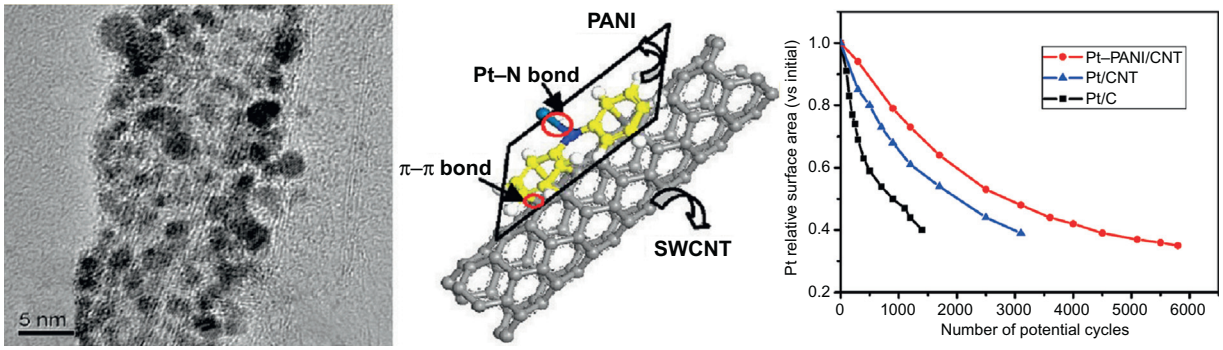

FIGURE 26.11 Molecular interactions of Pt−PANI/CNT electrocatalyst and their transmission electron microscopy image and ECSA for various potential cycles. *CNT*, carbon nanotube; *ECSA*, electrochemical surface area; *PANI*, polyaniline. *Reprinted from D. He, C. Zeng, C. Xu, N. Cheng, H. Li, S. Mu, et al., Polyaniline-functionalized carbon nanotube supported platinum catalysts, Langmuir 27 (2011) 5582−5588. Available from: https://doi.org/10.1021/la2003589. ©2011 American Chemical Society.*

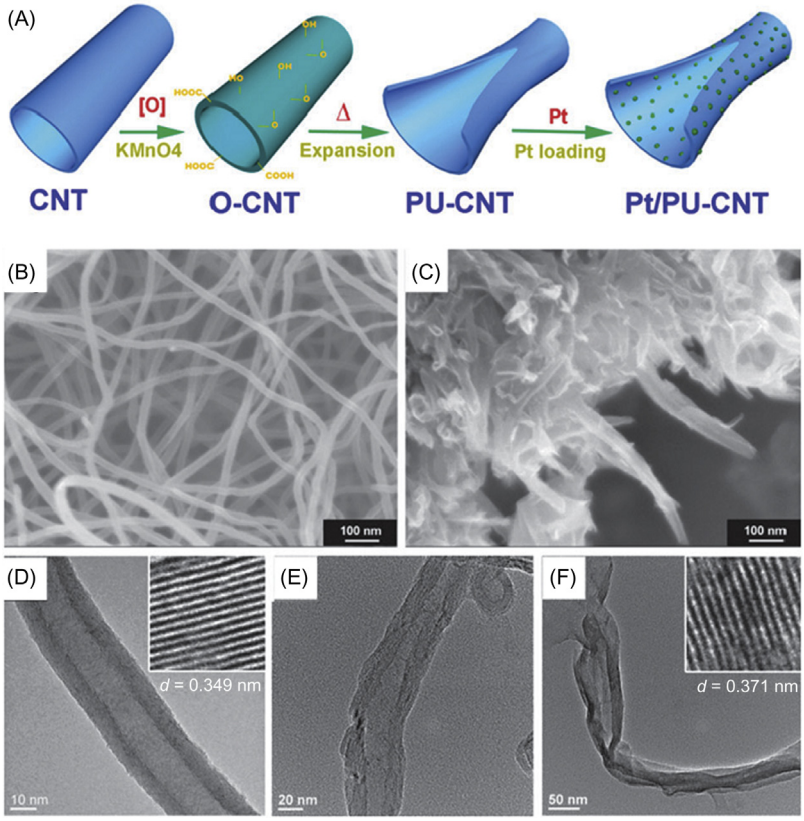

FIGURE 26.12 Schematic of the synthesis process of Pt/partially unzipped CNT (A) and the scanning electron microscopy images of CNTs (B), and partially unzipped CNTs (C), and transmission electron microscopy images of CNTs (D), O-CNTs (E), and partially unzipped CNTs (F). *CNT*, carbon nanotube. *Reprinted from D. Long, W. Li, W. Qiao, J. Miyawaki, S.-H. Yoon, I. Mochida, et al., Partially unzipped carbon nanotubes as a superior catalyst support for PEM fuel cells, Chem. Commun. 47 (2011) 9429−9431. Available from: https://doi.org/10.1039/c1cc13488d. ©2011 Royal Society of Chemistry.*

alloy-based nanomaterials supported on CNTs also have been used for improving the performance of cathode electrocatalyst in PEMFCs [154−156].

26.17 CARBON NANOFIBERS

CNFs are identified as more promising nanostructures which have been used in tremendous applications, including catalyst support, super capacitors, hydrogen storage, energy storage, etc. The major differences of CNFs over CNTs are the lack of a hollow cavity, bigger diameter, and longer length. These interestingly shaped materials possess stacking arrangements of graphene sheets having three classified structures of platelet, herringbone, and ribbon (Fig. 26.13) [157]. The CNFs have been synthesized mainly through various methods, including chemical vapor deposition and electrospinning [158−160]. Three types of Pt supported on CNFs with different ordering degree, diameter, and structure have been used to investigate the PEMFCs electrochemical activity [161].

Amongst all the methods, electrospinning is recognized as an easy and low-cost method that is more

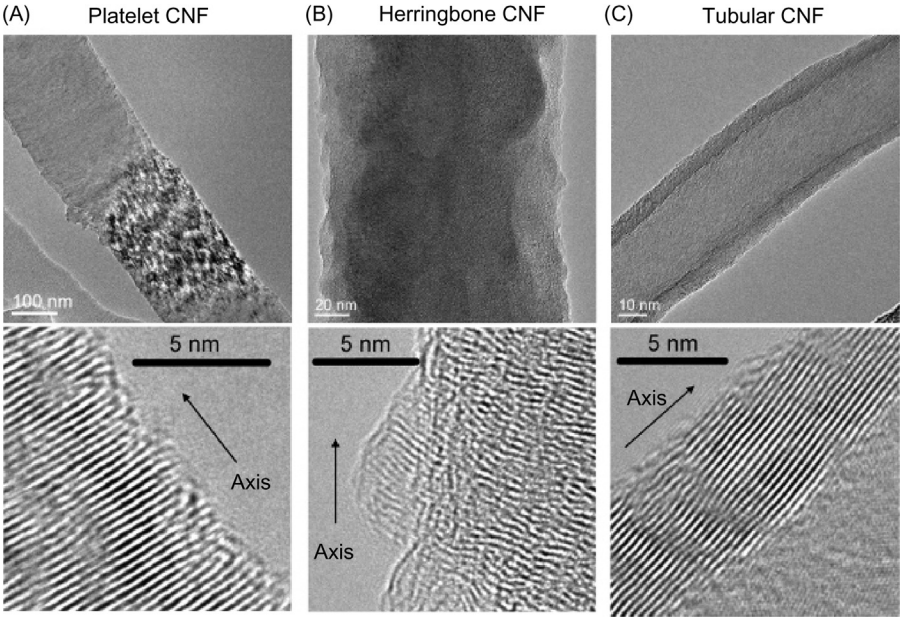

FIGURE 26.13 Transmission electron microscopy images of (A) platelet, (B) herringbone, and (C) tubular CNFs. *CNF*, carbon nanofiber. *Reprinted from M. Tsuji, M. Kubokawa, R. Yano, N. Miyamae, T. Tsuji, M.S. Jun, et al., Fast preparation of PtRu catalysts supported on carbon nanofibers by the microwave-polyol method and their application to fuel cells, Langmuir 23 (2007) 387–390. Available from: https://doi.org/10.1021/la062223u. ©2007 American Chemical Society.*

capable and feasible for producing extremely long nanofibers (~hundreds of kilometers if the process is continual) in large quantities with well-defined topologies. One of the crucial properties of these materials is their graphitic structure which facilitates higher thermal and electrical conductivities. In addition, they have more resistance to oxidation which makes them more durable support under high potential conditions in fuel cells. Li et al. [162] employed a polyol method to synthesize Pt nanoparticles supported on stacked-cup CNFs (SC-CNFs) for PEMFCs electrocatalyst and a unique filtration technique was used to develop Pt/SC-CNFs-based MEAs. An electrocatalyst with an optimized content of 50 wt.% Nafion ionomer displayed higher performance than the commercial black (E-TEK) with 30 wt.% Nafion. The results revealed that the high aspect ratio of conductive network in the Nafion matrix contributed to the performance enhancement. Similar to CNTs, CNFs require functionalization with harsh reagents such as HNO_3, H_2SO_4, etc., for the attachment of catalysts on the surface of the CNFs [163,164]. For instance, Li et al. reported the functionalization of CNFs using H_2SO_4 (4 M) and HNO_3 (2 M) at 100°C followed by ethylene glycol reduction method and found uniform distribution of Pt nanoparticles (2–4 nm) with loading range of 5–20 wt.% on outer walls of CNFs (Fig. 26.14). Furthermore, their experiment results also demonstrated that Pt loaded on CNFs with Nafion content of 50% showed better performance than Pt/CB with 30% Nafion [162].

Similarly, electrospun PAN-based CNFs were functionalized with HNO_3 and H_2SO_4 for 1, 3, and 5 hours followed by deposition of Pt nanoparticles onto the functionalized support. Even though the same catalyst loading was applied in all supports, 5 hours treated sample (294.7 mW/cm^2) showed maximum power density as compared to commercial Pt/C catalyst (151.8 mW/cm^2) which is due to the high surface area and more anchoring sites [163]. Another study conducted by [165] was to identify the effect of −COOH and −OH surface functional group on the activity of Pt electrocatalyst. The author found −OH containing CNFs have uniformly dispersed smaller particle size which exhibited better ORR activity (Fig. 26.15) than −COOH-treated CNFs.

Interestingly, Balan et al. reported the functionalization of CNFs by refluxing with H_2O_2 followed by Pt deposition. The functionalization of CNFs induced the formation of more anchoring sites which serves well distributed Pt nanoparticles (3 nm) into inner and outer walls of the nanofibers. Moreover, the effect of microstructure in CNFs on the ORR activity was thoroughly studied by Zheng et al. [166,167] who attempted to replace precious Pt catalyst with alternative electrocatalysts derived from iron, PANI, and polyacrylonitrile using thermal decomposition process The combined effect of porous structure (specific surface area 355 m^2/g) and nitrogen contents in conductive network of the nanofibers provides an enhancement in the ORR activity. Ren et al. [168] developed a core-shell structure of Fe_3C embedded nitrogen-doped CNFs from an electrospinning of $FeCl_3$ and polyvinylidene fluoride mixture followed by pyrolysis. Based on the results, they claimed that the synergetic effects between core-Fe_3C, pyrrolic N-doped graphite with porous structures of Fe_3C@NCNF (treated at 900°C) showed more efficient ORR performance (current density 4.79 mA/cm^2) and better durability (Fig. 26.16) in both acidic and alkaline medium which is slightly higher than that of Pt/C (4.45 mA/cm^2).

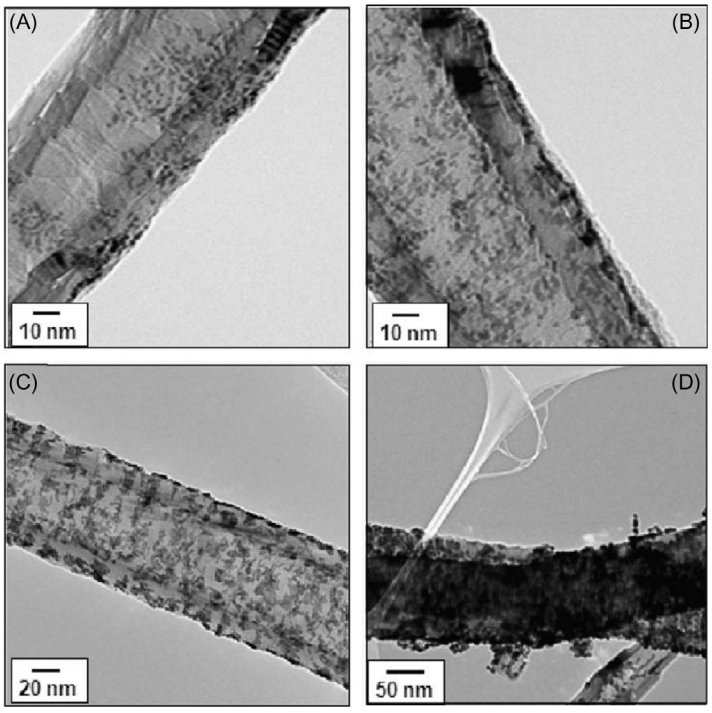

FIGURE 26.14 Transmission electron microscopy images of Pt/SC-CNFs with the metal loading of (A) 5 wt.%, (B) 10 wt.%, (C) 20 wt.%, and (D) 30 wt.%. *CNF*, carbon nanofiber; *SC-CNF*, stacked-cup CNF. *Reprinted from W. Li, M. Waje, Z. Chen, P. Larsen, Y. Yan, Platinum nanoparticles supported on stacked-cup carbon nanofibers as electrocatalysts for proton exchange membrane fuel cell, Carbon 48 (2010) 995–1003. Available from: https://doi.org/10.1016/j.carbon.2009.11.017. ©2010 Elsevier.*

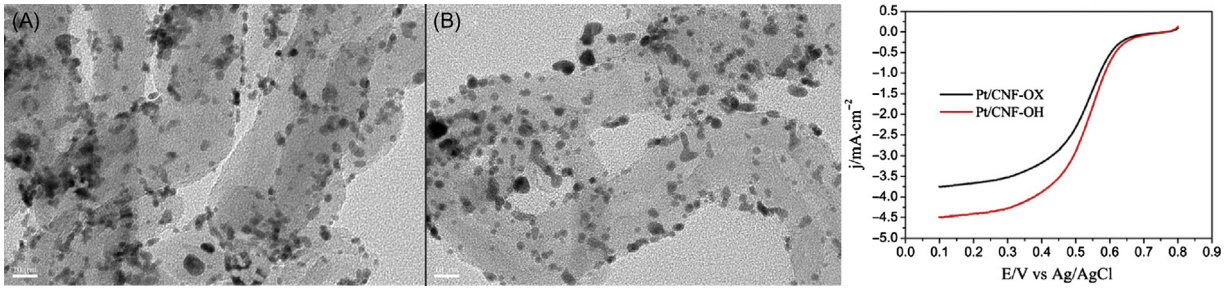

FIGURE 26.15 High resolution transmission electron microscopy images of Pt/CNF-OX (A) and Pt/CNF-OH (B) and their linear sweep voltammetry curve for ORR in O_2-saturated 0.5-M H_2SO_4 (C). $\upsilon = 10$ mV/s, $\omega = 1600$ rpm. *ORR*, oxygen reduction reaction; *CNF*, carbon nanofiber. *Reprinted from R.S. Zhong, Y.H. Qin, D.F. Niu, X.S. Zhang, X.G. Zhou, S.G. Sun, et al., Effect of carbon nanofiber surface groups on oxygen reduction reaction of supported Pt electrocatalyst, Electrochim. Acta 89 (2013) 157–162. Available from: https://doi.org/10.1016/j.electacta.2012.11.007. ©2013 Elsevier.*

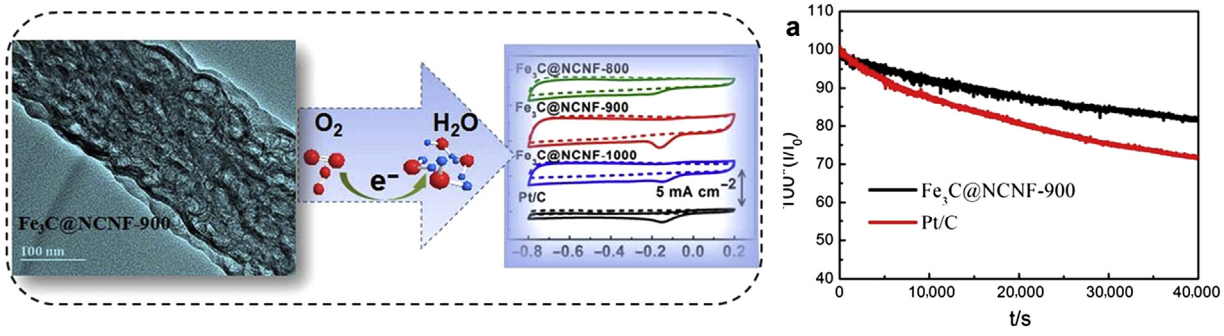

FIGURE 26.16 Electrocatalytic performance and durability studies of Fe_3C@NCNF-900 prepared using electrospinning and thermal treatment method. *Reprinted from G. Ren, X. Lu, Y. Li, Y. Zhu, L. Dai, L. Jiang, Porous core -shell Fe_3C embedded N-doped carbon nanofibers as an effective electrocatalysts for oxygen reduction reaction, ACS Appl. Mater. Interfaces 8 (2016) 4118–4125. Available from: https://doi.org/10.1021/acsami.5b11786. ©2016 American Chemical Society.*

Lin et al. [8] prepared CNFs supported with binary catalyst Pt−Pd by employing electrospinning and coelectrodeposition method. Their results showed that $Pt_{50}Pd_{50}$/CNFs performed as the best electrocatalytic support material for ORR in acidic medium. Interestingly, the combined effect of CNTs and CNFs was studied for ORR by [169]. Initially, Fe/CNF was obtained from carbonized electrospun nanofibers of $Fe(Ac)_2$/PAN and further subjected to CVD process by injecting toluene (for the CNT growth @750°C) or pyridine (for the NCNT growth @780°C) to grow N-doped CNT on CNFs (Fig. 26.17). By comparing NCNTs, CNT/CNFs, and commercial Pt/C catalyst, the study stated that NCNT/CNF composite performed as an effective electrocatalyst with long-term stability.

The ORR performance of Pt supported with nitrogen-doped CNFs were investigated by [170]. Oxygen and nitrogen containing groups were introduced in the CNFs by using sonochemical treatment carried out in the presence of mixed acids (H_2SO_4 and HNO_3) and ammonia. Based on their results, it was found that the ammonia-treated sample was showing good results as compared to acid-treated samples. This investigation suggested that the increased activity of Pt/CNF-ON is mainly attributed to the uniformly distributed smaller particle size and the presence of nitrogen containing groups. Zheng et al. [171] synthesized Ir−V nanoparticle supported on platelet CNFs using the chemical reduction method and the ORR results were compared with Ir−V supported on Vulcan XC-72. The Ir−V/CNFs showed higher current density (0.267 mA/cm^2) as compared to Ir−V/C. Similarly the Onset reduction potential for Ir−V/CNFs was about 0.53, while that of Ir−V/C was about 0.45 V and it was stated that the increase in activity might be because of the smaller particle size and the stronger interaction between metal particles and CNFs. Yuan et al. [172] followed a different method to prepare CNTs and CNFs support material from the catalytic decomposition of acetylene using Ni−MgO catalyst prepared by a mechanochemical (MC) process. The size and morphology of the CNTs and CNFs were tailored by grinding time in MC process and pyrolysis temperature in CVD process. The deposition of Pt catalyst (20 wt.%) on the as-prepared support material was carried out using polyol method. The twisted CNFs with smaller diameter (65 nm) gave the best performance with a fuel cell voltage of 645 mV at a current density of 500 mA/cm^2. Padmavathi et al. [163] reported the functionalization level optimization of electrospun CNF for PEMFCs application. The single-cell performance of Pt loaded on optimized nanofibers with SPEEK membrane showed maximum open circuit potential (0.863 V) and power density of 294.7 mW/cm^2 as compared to Pt/C (205.2 mW/cm^2) with Nafion membrane. Similarly, Zhong et al. [165] also studied the effect of carboxylic acid and hydroxyl functional groups of CNFs on ORR activity and their results indicated that hydroxyl group had better electrocatalytic activity. Karthikeyan and Biji [173] described the preparation of controlled mesopores (20−40 nm) with high specific surface area (724 m^2/g) CNFs using electrospinning and thermally induced phase separation method for PEMFC electrodes. The enhanced properties of the mesoporous CNFs could afford large number of active sites to improve the dispersion of Pt catalysts, making proper contact between the catalysts and the electrolyte by providing low resistance pathways and influencing the diffusivity of the electrolyte and reactant. Recently, Shin et al. [174] prepared nitrogen-doped CNFs with Co metal nanoparticles via electrospinning and pyrolysis method. The result shows the difference in electrocatalytic activity of CNFs and N-CNFs. The calculated

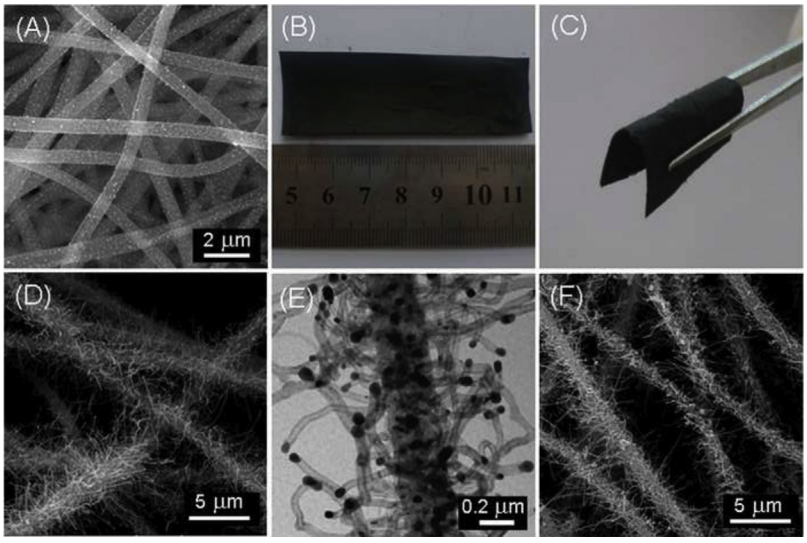

FIGURE 26.17 Scanning electron microscopy images of Fe/CNF (A), NCNT/CNFs (D), and CNT/CNFs (F), and optical photos of NCNT/CNFs film with good mechanical flexibility (B and C), and (E) is the transmission electron microscopy image of NCNT/CNFs. *CNT*, carbon nanotube; *CNF*, carbon nanofiber. *Reprinted from Q. Guo, D. Zhao, S. Liu, S. Chen, M. Hanif, H. Hou, Free-standing nitrogen-doped carbon nanotubes at electrospun carbon nanofibers composite as an efficient electrocatalyst for oxygen reduction, Electrochim. Acta 138 (2014) 318−324. Available from: https://doi.org/10.1016/j.electacta.2014.06.120. ©2014 Elsevier.*

electron transfer number of ORR for Co−N-CNFs electrocatalyst is 3.70 which is almost similar to Pt/C (3.85). Similarly, Jiang et al. [170] used nitrogen- and oxygen-doped synthesized CNFs using acid and ammonia treatment from the ultrasonic method. The ammonia treated sample showed higher ECSA, diffusion limiting current density, and more positive (40 mV) half wave potential in ORR as compared to acid treated CNFs.

26.18 GRAPHENE

In recent years, graphene-based nanomaterials have got great interest as catalyst support materials for polymer electrolyte membrane (PEM) fuel cell, especially for ORRs [175,176]. Chemically synthesized graphene possesses surface functional groups (carbonyls, epoxides, hydroxyls, etc.) and contains lattice defects in the interlayer structure of graphene (vacancies, holes). These functionalities and lattice defects can anchor and immobilize the metal nanoparticles with strong metal−support interaction; thereby the stability of electrocatalysts can be enhanced for specific applications. So far, graphene structures have been engineered by different routes to attain high performance in fuel cells. Hsieh et al. synthesized highly crystalline platinum nanoclusters graphene nanosheets by employing a pulse electrochemical deposition method for studying the performance of PEMFCs [177]. Recently, Lu et al. [125] described the preparation of PtPd catalysts supported on graphene and observed enhanced electrocatalytic activity and more stability as compared to commercial catalyst (Pt/C). Carbon atoms in the hexagonal honeycomb lattice of graphene can be replaced by doping with foreign hetero atoms, such as boron, nitrogen, phosphorous, sulfur, iodine, etc. The most commonly used synthesis method for doping of graphene are CVD [178], arc-discharge [179], pyrolysis [180], plasma treatment [117], solvothermal [120], hydrothermal [118], thermal annealing [119]. Interestingly Wen et al. [121] studied the performance of microbial fuel cells cathodes from electrocatalysts consisting of graphene embedded with porous nitrogen-doped carbon and found higher electrochemical activity compared to Pt/C catalysts. Wet-chemical approach was employed by [21,22] to prepare Pt−Pd nanodendrites supported on graphene nanosheets for fuel cell applications. The synthesis method of graphene nanosheet/Pt−Pd bimetallic nanodendrite is shown in Fig. 26.18. Initially, the exfoliated graphene oxide samples were functionalized with PVP, and further treated with H_2PdCl_4 and HCOOH to form graphene/Pd hybrid material. The hybrid material was further treated with PVP solution, ascorbic acid and K_2PtCl_4 to convert graphene nanosheet/Pt−Pd bimetallic nanodendrite. The results showed that smaller sized Pt nanobranches were supported on Pd NCs with porous structure

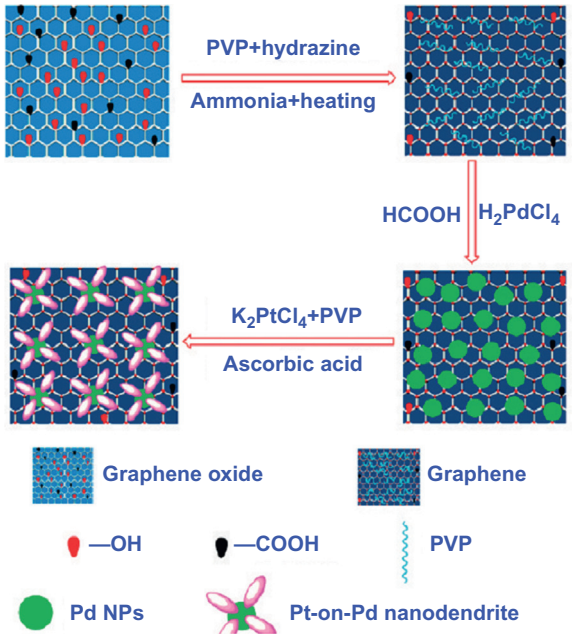

FIGURE 26.18 Synthesis procedure of graphene nanosheet/Pt on Pd bimetallic nanodentrite hybrids. *Reprinted from L. Guo, V.M. Swope, B. Merzougui, L. Protsailo, M. Shao, Q. Yuan, et al., Oxidation resistance of bare and Pt-coated electrically conducting diamond powder as assessed by thermogravimetric analysis, J. Electrochem. Soc. 157 (2010) A19. Available from: https://doi.org/10.1149/1.3246410; S. Guo, S. Dong, E. Wang, Three-dimensional Pt-on-Pd bimetallic nanodendrites supported on graphene nanosheet: facile synthesis and used as an advanced nanoelectrocatalyst for methanol oxidation, ACS Nano 4 (2010) 547−555. Available from: https://doi.org/10.1021/nn9014483. ©2010 American Chemical Society.*

which were directly grown onto the surface of graphene nanosheets. Moreover, they claimed that the electrocatalytic performance of the bimetallic nanodendrites with controllable size or different numbers of Pt branches adhering to graphene nanosheets have much higher catalytic activity than conventional E-TEK Pt/C.

26.19 ORDERED MESOPOROUS CARBON

According to the IUPAC nomenclature the pore size between 2 and 50 nm is called mesopores. Based on the structures and morphologies, the mesoporous carbon (with pore sizes from 2 to 50 nm) can be divided into two types: OMC (typically synthesized by nanocasting or direct templating method) and disordered mesoporous carbon (DOMC). So far, different synthesis methods have been widely employed for preparing mesoporous carbon materials as catalyst supports for PEMFCs [74,75,122,181]. The two most extensively used methods for preparing OMCs are hard-template (e.g., SBA-15, MCM-41, and silica colloid) and soft-template (e.g., amphiphilic surfactants and triblock copolymers). In the hard-template method, pores in OMS are mixed with a

carbon source such as sucrose, resorcinol, or formaldehyde. The OMCs are obtained by subjecting into carbonization followed by the removal of the silica template. In the soft-template method, the carbon precursors are usually organic monomers which are polymerized with the self-assembly of a surfactant in a liquid to form a carbon−surfactant composite. The complete removal of surfactant and further carbonization yield OMCs. Schematic diagrams of the both hard-template and soft-template method are shown in Fig. 26.19 [182].

The study by [183] suggested that the presence of 3D interconnected porous structure in mesoporous carbon facilitating the electrical conductivity, mass transfer, and uniform dispersion of the catalyst particles. The catalysts [Pt/Pt-alloy (or) non-Pt-based catalyst] supported on mesoporous carbon have shown improved overall performance in PEMFCs. For achieving high performance, the fuel cell electrode must have more triple-phase boundary sites. But conventional carbon support (carbon black) contains only micropores (<2 nm) and deep cracks which reduces the complete utilization of catalyst particles [improper network between reactants and proton conducting electrolyte (e.g., Nafion) due to the smaller pore size]. Moreover, the larger pore sizes (>50 nm) of support materials have low specific surface area and less electrical conductivity [42,184]. Yu et al. [185] demonstrated that PtRu catalysts supported on porous carbon with mesopore size of 25 nm showed an excellent performance compared to commercial catalyst material (E-TEK). This performance enhancement was not only due to larger pore volume and higher surface area, but, also facilitated a larger amount of uniform catalyst dispersion, ordered interconnected pore structures (proper transport of reactants and products). The above study suggested that the performances of the supported catalysts depend on both pore sizes, pore structure, electrical conductivity. Although DOMC structure contains mesoporosity, it failed to meet the support characteristics, such as electrical conductivity, specific surface area, and mass transport, which is mainly due to the isolated and irregularly interconnected structures. Moreover, the electrical conductivity of the Pt supported on mesoporous carbon is lower than that of Vulcan XC-72. But, the electrical conductivity also can be improvised from the aromatic carbon precursors, annealing temperature, and catalytic graphitization. Joo et al. [185a] initiated the application of OMC materials for fuel cells application and they prepared uniformly dispersed catalyst (Pt) nanoparticles onto hexagonally mesostructured tube-type CMK-5 carbon by impregnation method using Pt precursor (H_2PtCl_6) and subsequent reduction with H_2 gas. They found very much smaller particle size (3 nm) and high catalytic activity toward ORR which is comparably superior to the conventional supports, such as carbon black, activated carbon, and activated carbon fibers. The results suggested that the high catalytic activity is mainly attributed to the high metal dispersion and mesoporous structure of the CMK-5 carbon support. Ding et al. [186] prepared OMC supported catalysts from different approaches. In which the cathode catalyst (Pt nanoparticles) were predeposited onto the silica template prior to the formation of the carbon structure. In the case of an anode catalyst PtRu, the polyol method was adopted and subsequently, PtRu colloid was adsorbed onto OMC support. Even though the particle size of the Pt/CMK-3 catalyst was bigger than the commercial catalyst, 10 wt.% Pt supported Pt/CMK-3 electrocatalyst displayed improved activity for the ORR. Pt supported with mesoporous carbon material was

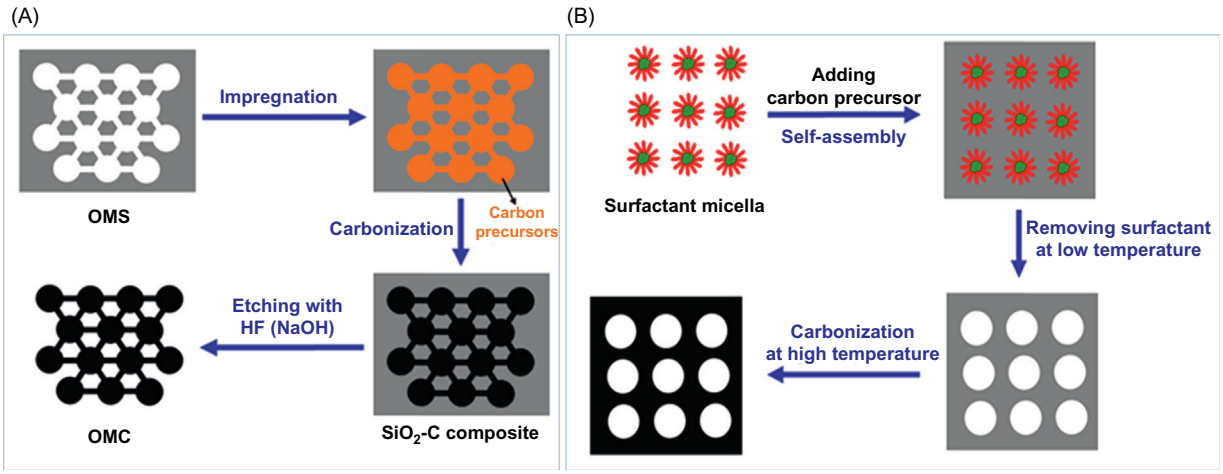

FIGURE 26.19 Schematic diagrams of (A) hard template and (B) soft template methods to prepare mesoporous carbon. *Reprinted from K.L. Yeung, W. Han, Zeolites and mesoporous materials in fuel cell applications, Catal. Today 236 (2014) 182−205. Available from: https://doi.org/10.1016/j.cattod.2013.10.022. ©2014 Elsevier.*

prepared by [187] which shows higher mass specific kinetic current density and durability than commercial catalyst. Viva et al. [188] prepared mesoporous carbon support (pore size 20 nm and a pore volume of 0.99 cm^3/g) with Pt catalyst by impregnation method. Mesoporous-based electrocatalyst showed lower over potential and lesser peroxide (H_2O_2) generation with a yield of 0.25% in ORR, which is much lower than the yield of 1.25% from Pt/C. Recently, Banham et al. [189] studied the importance of the OMC support dimensions (as opposed to the pore diameter) on ORR activity of Pt/OMC catalysts and found wall thickness of OMC is playing a crucial role in the activity [190]. Ahn et al. [191] prepared Pt/OMC using nanoreplication followed by incipient wetness method and also investigated the effect of ionomer content for the optimum activity (Fig. 26.20). They found that Pt/OMCs require less ionomer (10 wt.%) than catalysts based on carbon black support (20 and 30 wt.%).

Besides, Wang et al. [117] prepared ammonia-treated OMC (nitrogen-doped) elctrocatalyst for ORR in acidic media and found higher activity compared to commercial material. Liu et al. [191a] reported the preparation of Pt on OMC support material using organic−organic self-assembly approach and results suggested that the mesoporous carbon effectively precludes migration and/or agglomeration of Pt nanoparticles which increased the activity and durability. Graphitized OMC studded with metals such as Fe, CO, and Ni were synthesized by [192] by using M-SBA template for PEMFCs electrocatalyst support. The fuel cell polarization result shows that Pt/Ni-OMC performed better than Pt/OMC among other transition metal modified graphitized mesoporous carbon which is due to the presence of defective graphitic structure. Similarly, Cheon et al. [193] prepared ordered mesoporous porphyrinic carbons (OMPC) (Fig. 26.21) and they presented the electrocatalytic performance of nonprecious metal catalysts based on OMPCs with metals, such as Fe, CO, FeCo. The FeCo catalysts supported OMPC showed better performance and high durability in acidic medium compared to other nonprecious catalysts which indicates

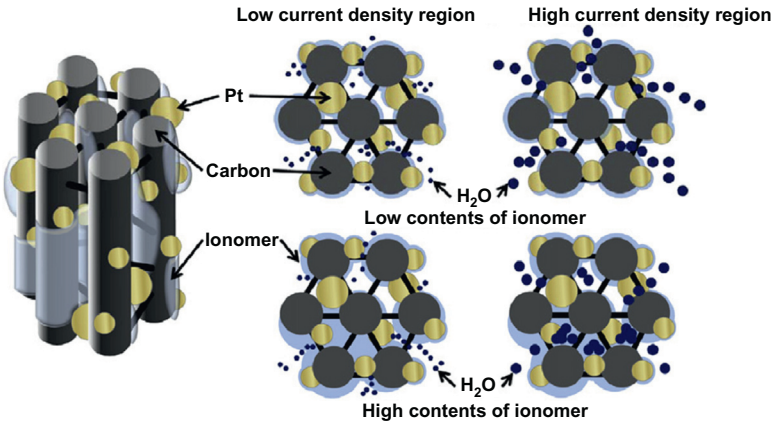

FIGURE 26.20 A schematic illustration for the effect of ionomer contents in the low and high current density regions. *Reprinted from C.Y. Ahn, J.Y. Cheon, S.H. Joo, J. Kim, Effects of ionomer content on Pt catalyst/ordered mesoporous carbon support in polymer electrolyte membrane fuel cells, J. Power Sources 222 (2013) 477−482. Available from: https://doi.org/10.1016/jjpowsour.2012.09.012. ©2013 Elsevier.*

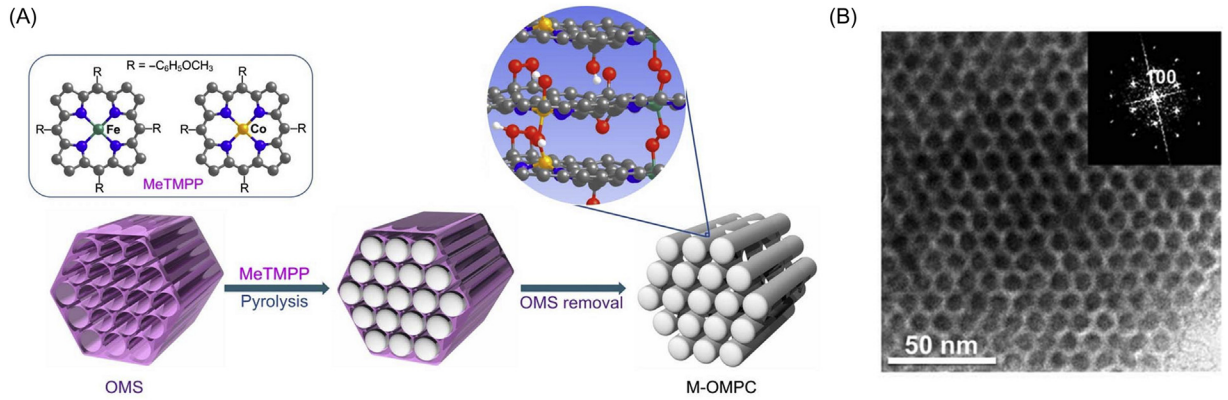

FIGURE 26.21 (A) Schematic synthetic strategy and (B) transmission electron microscopy image of M-OMPC catalysts synthesized via a nanocasting method that employed OMSs as templates and metalloporphyrins as the carbon source. *OMPC*, ordered mesoporous porphyrinic carbons. *Reprinted from J.Y. Cheon, T. Kim, Y. Choi, H.Y. Jeong, M.G. Kim, Y.J. Sa, et al., Ordered mesoporous porphyrinic carbons with very high electrocatalytic activity for the oxygen reduction reaction, Sci. Rep. (2013) 1-8. Available from: https://doi.org/10.1038/srep02715. ©2013 Nature.*

its weak interaction with oxygen, high density of active sites, and the use of porphyrin precursors.

26.20 BORON-DOPED DIAMOND

It is well-known that the electrical conductivity of diamond increases upon doping with most common elements, such as boron, phosphorous, or nitrogen. The lowest activation energy (0.37 eV) of boron is more ideal dopant in comparison with other elements. Moreover, boron-doped diamond (BDD) is highly favorable for fuel cell catalyst support material due to high electrochemical stability and corrosion resistance in both alkaline and acidic conditions. Particularly, this electrochemical corrosion in the support material causes high electrical resistance which leads to weakening of the interactions of the catalyst particles and support surface. For this particular argument, BDD can be an alternative support material. Typically, different routes have applied to deposit the catalysts onto BDD such as implantation [194], thermal decomposition, and codeposition using CVD and electrochemical deposition [194–196]. Salazar-Banda et al. [196a] reported the preparation of BDD support material from grinding of BDD, and the Pt catalyst was supported using the sol–gel method. Salazar-Banda et al. [196b] synthesized the electrocatalysts including Pt, Pt–RuO_2, Pt–RuO_2–RhO_2, Pt–SnO_2, and Pt–Ta_2O_5 on BDD using sol–gel method. Their results obtained from BDD supported electrocatalysts exhibited excellent performance toward electrochemical stability and corrosion resistance. Kim et al. [72,73] prepared BDD (~200 nm size) by electrostatic self-assembly method and they investigated the morphological changes of support material during the real operating conditions of PEMFCs. The accelerated long-term stability study showed that Pt/BDD showed more stable performance which implied that Pt detachment was not occurring during long cycle operation. Similarly, Swain et al. [196c] prepared support material by overcoating of high surface area diamond powder with thin layer of BDD. The reported results indicated that Pt supported on BDD was more resistant to oxygen compared to commercial catalysts. However, under real operating conditions, it is very difficult to recognize the durability and degradation mechanisms of platinum supported on BDD. Electrophoretic technique was employed for the deposition of Pt nanoparticles on nanodiamond support but, agglomeration was observed [197]. The dopants are more advantageous for enhancing the electrical conductivity in diamonds. Meanwhile, these dopants conversely deteriorate the stability of the support material. Based on that, there was an interesting study conducted by [198] in which they demonstrated Pd supported on insulating, highly crystalline diamond as an alternative catalyst support material for fuel cell. They also claimed that these catalyst support materials can even possibly be applied in conditions such as high temperature and high pressure.

The utilization of carbon-based nanostructure materials has unquestionably shown an improved performance and better durability as the catalyst support material. But still, carbon corrosion is deficient in these PEMFC systems which affects the overall performance. Though the carbon corrosion is regarded as a significant reaction problem, the complete exclusion of carbon corrosion has not yet been practicable. Moreover, functionalization of the carbon support is necessarily to be used to bind the catalyst nanoparticles, which in turn leads to loss of electrochemical active surface area. This also can diminish the ionomer distribution thus affecting proton conductivity in the fuel cell electrodes. Consequently, there is a need to make an attempt to prepare alternative supports to overcome these issues.

REFERENCES

[1] R. O'Hayre, D.M. Barnett, F.B. Prinz, The triple phase boundary, J. Electrochem. Soc. 152 (2005) A439. Available from: https://doi.org/10.1149/1.1851054.

[2] G. Centi, M. Gangeri, M. Fiorello, S. Perathoner, J. Amadou, D. Bégin, et al., The role of mechanically induced defects in carbon nanotubes to modify the properties of electrodes for PEM fuel cell, Catal. Today 147 (2009) 287–299.

[3] S. Du, B. Millington, B.G. Pollet, The effect of Nafion ionomer loading coated on gas diffusion electrodes with in situ grown Pt nanowires and their durability in proton exchange membrane fuel cells, Int. J. Hydrogen Energy 36 (2011) 4386–4393.

[4] L. Wang, S.G. Advani, A.K. Prasad, Membrane electrode assembly with enhanced membrane/electrode interface for proton exchange membrane fuel cells, J. Phys. Chem. C 117 (2013) 945–948.

[5] C. Wang, Preparation of a self-humidifying membrane electrode assembly for fuel cell and its performance analysis, Sci. China, Ser. G 46 (2003) 501.

[6] G.P. Henry, A.A. Robert, U.S. Pat.; 4,044,193, 1973.

[7] E.I. Santiago, L.C. Varanda, H.M. Villullas, Carbon-supported Pt–Co catalysts prepared by a modified polyol process as cathodes for PEM fuel cells, J. Phys. Chem. C 111 (2007) 3146–3151.

[8] Z. Lin, L. Ji, O. Toprakci, W. Krause, X. Zhang, Electrospun carbon nanofiber-supported Pt–Pd alloy composites for oxygen reduction, J. Mater. Res. 25 (2010) 1329. Available from: https://doi.org/10.1557/JMR.2010.016.

[9] S.A. Grigoriev, P. Millet, V.N. Fateev, Evaluation of carbon-supported Pt and Pd nanoparticles for the hydrogen evolution reaction in PEM water electrolysers, J. Power Sources 177 (2008) 281–285.

[10] N. Rajalakshmi, H. Ryu, M.M. Shaijumon, S. Ramaprabhu, Performance of polymer electrolyte membrane fuel cells with carbon nanotubes as oxygen reduction catalyst support material, J. Power Sources 140 (2005) 250–257.

[11] A. Caillard, C. Charles, R. Boswell, P. Brault, Integrated plasma synthesis of efficient catalytic nanostructures for fuel cell, Nanotechnology 18 (2007) 305603.

[12] G. Chen, S.R. Bare, T.E. Mallouk, Development of supported bifunctional electrocatalysts for unitized regenerative fuel cells, J. Electrochem. Soc. 149 (2002) A1092. Available from: https://doi.org/10.1149/1.1491237.

[13] D. Gruber, J. Müller, Enhancing PEM fuel cell performance by introducing additional thin layers to sputter-deposited Pt catalysts, J. Power Sources 171 (2007) 294–301.

[14] V. Raghuveer, A. Manthiram, A.J. Bard, Pd–Co–Mo electrocatalyst for the oxygen reduction reaction in proton exchange membrane fuel cells, J. Phys. Chem. B 109 (2005) 22909–22912.

[15] V.M. Dhavale, S. Kurungot, Tuning the performance of low-Pt polymer electrolyte membrane fuel cell electrodes derived from Fe_2O_3@Pt/C core—

shell catalyst prepared by an in situ anchoring strategy, J. Phys. Chem. C 116 (2012) 7318−7326,.
[16] Y. Song, R.M. Garcia, R.M. Dorin, H. Wang, Y. Qiu, E.N. Coker, et al., Synthesis of platinum nanowire networks using a soft template, Nano Lett. 7 (2007) 3650−3655.
[17] H. Lee, S. Choi, S.M. Jo, D.Y. Kim, S. Kwak, M.W. Cha, et al., Fabrication and electrical properties of platinum nanofibres by electrostatic spinning, J. Phys. D: Appl. Phys. 42 (2009) 125409.
[18] H. Ahn, W. Jin, T. Seong, D. Wang, Three-dimensional nanostructured carbon nanotube array/PtRu nanoparticle electrodes for micro-fuel cells, Electrochem. Commun. 11 (2009) 635−638.
[19] H. Yin, H. Tang, D. Wang, Y. Gao, Z. Tang, Facile synthesis of surfactant-free Au cluster/graphene hybrids for high-performance oxygen reduction reaction different shapes of Pt catalysts, ACS Nano 6 (2012) 8288−8297.
[20] G.Y. Zhao, C.L. Xu, D.J. Guo, H. Li, H.L. Li, Template preparation of Pt−Ru and Pt nanowire array electrodes on a Ti/Si substrate for methanol electro-oxidation, J. Power Sources 162 (2006) 492−496.
[21] L. Guo, V.M. Swope, B. Merzougui, L. Protsailo, M. Shao, Q. Yuan, et al., Oxidation resistance of bare and Pt-coated electrically conducting diamond powder as assessed by thermogravimetric analysis, J. Electrochem. Soc. 157 (2010) A19. Available from: https://doi.org/10.1149/1.3246410.
[22] S. Guo, S. Dong, E. Wang, Three-dimensional Pt-on-Pd bimetallic nanodendrites supported on graphene nanosheet: facile synthesis and used as an advanced nanoelectrocatalyst for methanol oxidation, ACS Nano 4 (2010) 547−555. Available from: https://doi.org/10.1021/nn9014483.
[23] X. Zhang, W. Lu, J. Da, H. Wang, D. Zhao, P.A. Webley, Porous platinum nanowire arrays for direct ethanol fuel cell applications, Chem. Commun. 0 (2009) 195−197.
[24] X. Yan, S. Kwon, A.M. Contreras, J. Bokor, G.A. Somorjai, Fabrication of large number density platinum nanowire arrays by size reduction lithography and nanoimprint lithography, Nano Lett. 5 (2005) 8−11.
[25] H. Peng, Z. Mo, S. Liao, H. Liang, L. Yang, F. Luo, et al., High performance Fe- and N-doped carbon catalyst with graphene structure for oxygen reduction, Sci. Rep. 3 (2013) 1765.
[26] S.M. Choi, J.H. Kim, J.Y. Jung, E.Y. Yoon, W.B. Kim, Pt nanowires prepared via a polymer template method: its promise toward high Pt-loaded electrocatalysts for methanol oxidation, Electrochim. Acta 53 (2008) 5804−5811.
[27] S.X. Lu, K. Sivakumar, B. Panchapakesan, Sonochemical synthesis of platinum nanowires and their applications as electro-chemical actuators, J. Nanosci. Nanotechnol. 7 (2007) 2473−2479.
[28] H. Zhou, W. Zhou, R.R. Adzic, S.S. Wong, Enhanced electrocatalytic performance of one-dimensional metal nanowires and arrays generated via an ambient, Surfactantless Synth. 4 (2009) 5460−5466.
[29] X. Teng, M. Feygenson, Q. Wang, J. He, W. Du, A.I. Frenkel, et al., Electronic and magnetic properties of ultrathin Au/Pt nanowires 2009, Nano Lett. 9 (2009) 3177−3184.
[30] J. Xie, Q. Zhang, W. Zhou, J.Y. Lee, D.I.C. Wang, Template-free synthesis of porous platinum networks of different morphologies, Langmuir 25 (2009) 6454−6459.
[31] Z. Chen, M. Waje, W. Li, Y. Yan, Supportless Pt and PtPd nanotubes as electrocatalysts for oxygen-reduction reactions, Angew. Chem. Int. Ed. 46 (2007) 4060−4063.
[32] D. Fenske, H. Borchert, J. Kehres, R. Kro, J. Parisi, Colloidal synthesis of Pt nanoparticles: on the formation and stability of nanowires, Langmuir 24 (2008) 9011−9016.
[33] C. Lee, X. Wei, J.W. Kysar, J. Hone, Measurement of the elastic properties and intrinsic strength of monolayer graphene, Science 321 (2008) 385−388. Available from: https://doi.org/10.1126/science.1157996.
[34] S. Sun, F. Jaouen, J.P. Dodelet, Controlled growth of Pt nanowires on carbon nanospheres and their enhanced performance as electrocatalysts in PEM fuel cells, Adv. Mater. 20 (2008) 3900−3904.
[35] M. Liu, R. Zhang, W. Chen, Graphene-supported nanoelectrocatalysts for fuel cells: synthesis, properties, and applications, Chem. Rev. 114 (2014) 5117−5160.
[36] S.-Y. Huang, P. Ganesan, B.N. Popov, Titania supported platinum catalyst with high electrocatalytic activity and stability for polymer electrolyte membrane fuel cell, Appl. Catal., B 102 (2011) 71−77. Available from: https://doi.org/10.1016/j.apcatb.2010.11.026.
[37] K.A. Hengge, C. Heinzl, M. Perchthaler, S. Geiger, K.J.J. Mayrhofer, C. Scheu, et al., Growth of porous platinum catalyst structures on tungsten oxide support materials: a new design for electrodes, Cryst. Growth Des. (2017). doi:10.1021/acs.cgd.6b01663.
[38] M.A. Hoque, D.C. Higgins, F.M. Hassan, J.-Y. Choi, M.D. Pritzker, Z. Chen, Tin oxide—mesoporous carbon composites as platinum catalyst supports for ethanol oxidation and oxygen reduction, Electrochim. Acta 121 (2014) 421−427. Available from: https://doi.org/10.1016/j.electacta.2013.12.075.
[39] B. Seger, A. Kongkanand, K. Vinodgopal, P.V. Kamat, Platinum dispersed on silica nanoparticle as electrocatalyst for PEM fuel cell, J. Electroanal. Chem. 621 (2008) 198−204. Available from: https://doi.org/10.1016/j.jelechem.2007.09.037.
[40] H. Chhina, S. Campbell, O. Kesler, An oxidation-resistant indium tin oxide catalyst support for proton exchange membrane fuel cells, J. Power Sources 161 (2006) 893−900. Available from: https://doi.org/10.1016/j.jpowsour.2006.05.014.
[41] Y. Fovet, J.Y. Gal, F. Toumelin-Chemla, Influence of pH and fluoride concentration on titanium passivating layer: Stability of titanium dioxide, Talanta 53 (2001) 1053−1063. Available from: https://doi.org/10.1016/S0039-9140(00)00592-0.
[42] E. Antolini, Carbon supports for low-temperature fuel cell catalysts, Appl. Catal., B 88 (2009) 1−24. Available from: https://doi.org/10.1016/j.apcatb.2008.09.030.
[43] F. Leroux, P.J. Dewar, M. Intissar, G. Ouvrard, L.F. Nazar, Study of the formation of mesoporous titania via a template approach and of subsequent Li insertion, J. Mater. Chem. 12 (2002) 3245−3253. Available from: https://doi.org/10.1039/B204051D.
[44] I.I. Vlasov, O.I. Lebedev, V.G. Ralchenko, E. Goovaerts, G. Bertoni, G. Van Tendeloo, et al., Hybrid diamond−graphite nanowires produced by microwave plasma chemical vapor deposition, Adv. Mater. 19 (2007) 4058−4062. Available from: https://doi.org/10.1002/adma.200700442.
[45] T. Ioroi, Z. Siroma, N. Fujiwara, S.I. Yamazaki, K. Yasuda, Sub-stoichiometric titanium oxide-supported platinum electrocatalyst for polymer electrolyte fuel cells, Electrochem. Commun. 7 (2005) 183−188. Available from: https://doi.org/10.1016/j.elecom.2004.12.007.
[46] D.V. Bavykin, J.M. Friedrich, F.C. Walsh, Protonated titanates and TiO_2 nanostructured materials: synthesis, properties, and applications, Adv. Mater. 18 (2006) 2807−2824. Available from: https://doi.org/10.1002/adma.200502696.
[47] M. Gustavsson, H. Ekström, P. Hanarp, L. Eurenius, G. Lindbergh, E. Olsson, et al., Thin film Pt/TiO_2 catalysts for the polymer electrolyte fuel cell, J. Power Sources 163 (2007) 671−678. Available from: https://doi.org/10.1016/j.jpowsour.2006.10.005.
[48] B.E. Hayden, D.V. Malevich, D. Pletcher, Electrode coatings from sprayed titanium dioxide nanoparticles—behaviour in NaOH solutions, Electrochem. Commun. 3 (2001) 390−394. Available from: https://doi.org/10.1016/S1388-2481(01)00181-3.
[49] W.X. Chen, J.Y. Lee, Z.L. Liu, Microwave-assisted synthesis of carbon supported Pt nanoparticles for fuel cell applications, Chem. Commun. 21 (2002) 2588−2589.
[50] S.-Y. Huang, P. Ganesan, B.N. Popov, Electrocatalytic activity and stability of titania-supported platinum−palladium electrocatalysts for polymer electrolyte membrane fuel cell, ACS Catal. 2 (2012) 825−831. Available from: https://doi.org/10.1016/j.apcatb.2010.11.026.
[51] D.S. Kim, E.F.A. Zeid, Y.T. Kim, Additive treatment effect of TiO_2 as supports for Pt-based electrocatalysts on oxygen reduction reaction activity, Electrochim. Acta 55 (2010) 3628−3633. Available from: https://doi.org/10.1016/j.electacta.2010.01.055.
[52] E. Formo, E. Lee, D. Campbell, Y. Xia, Functionalization of electrospun TiO_2 nanofibers with Pt nanoparticles and nanowires for catalytic applications, Nano Lett. 8 (2008) 668−672. Available from: https://doi.org/10.1021/nl073163v.
[53] G. Wu, M.A. Nelson, N.H. Mack, S. Ma, P. Sekhar, F.H. Garzon, et al., Titanium dioxide-supported non-precious metal oxygen reduction electrocatalyst, Chem. Commun. 46 (2010) 7489. Available from: https://doi.org/10.1039/c0cc03088k.
[54] K. Tiido, N. Alexeyeva, M. Couillard, C. Bock, B.R. MacDougall, K. Tammeveski, Graphene-TiO_2 composite supported Pt electrocatalyst for oxygen reduction reaction, Electrochim. Acta 107 (2013) 509−517. Available from: https://doi.org/10.1016/j.electacta.2013.05.155.
[55] W. Zhuang, L. He, J. Zhu, R. An, X. Wu, L. Mu, et al., TiO_2 nanofibers heterogeneously wrapped with reduced graphene oxide as efficient Pt electrocatalyst

supports for methanol oxidation, Int. J. Hydrogen Energy 40 (2015) 3679–3688. Available from: https://doi.org/10.1016/j.ijhydene.2015.01.042.

[56] Z. Huang, R. Lin, R. Fan, Q. Fan, J. Ma, Effect of TiB_2 pretreatment on Pt/TiB_2 catalyst performance, Electrochim. Acta 139 (2014) 48–53. Available from: https://doi.org/10.1016/j.electacta.2014.06.144.

[57] T. Xu, H. Zhang, H. Zhong, Y. Ma, H. Jin, Y. Zhang, Improved stability of TiO_2 modified Ru85Se15/C electrocatalyst for proton exchange membrane fuel cells, J. Power Sources 195 (2010) 8075–8079. Available from: https://doi.org/10.1016/j.jpowsour.2010.07.019.

[58] Q. Du, J. Wu, H. Yang, Pt@Nb–TiO_2 catalyst membranes fabricated by electrospinning and atomic layer deposition, ACS Catal. 4 (2014) 144–151. Available from: https://doi.org/10.1021/cs400944p.

[59] T. Oh, J.Y. Kim, Y. Shin, M. Engelhard, K.S. Weil, Effects of tungsten oxide addition on the electrochemical performance of nanoscale tantalum oxide-based electrocatalysts for proton exchange membrane (PEM) fuel cells, J. Power Sources 196 (2011) 6099–6103. Available from: https://doi.org/10.1016/j.jpowsour.2011.03.058.

[60] N.G. Akalework, C.-J. Pan, W.-N. Su, J. Rick, M.-C. Tsai, J.-F. Lee, et al., Ultrathin TiO_2-coated MWCNTs with excellent conductivity and SMSI nature as Pt catalyst support for oxygen reduction reaction in PEMFCs, J. Mater. Chem. 22 (2012) 20977. Available from: https://doi.org/10.1039/c2jm34361d.

[61] B. Basu, G.B. Raju, A.K. Suri, Processing and properties of monolithic TiB_2 based materials, Int. Mater. Rev. 51 (2006) 352–374. Available from: https://doi.org/10.1179/174328006X102529.

[62] S. Yin, S. Mu, H. Lv, N. Cheng, M. Pan, Z. Fu, A highly stable catalyst for PEM fuel cell based on durable titanium diboride support and polymer stabilization, Appl. Catal., B 93 (2010) 233–240. Available from: https://doi.org/10.1016/j.apcatb.2009.09.034.

[63] S. Yin, S. Mu, M. Pan, Z. Fu, A highly stable TiB_2-supported Pt catalyst for polymer electrolyte membrane fuel cells, J. Power Sources 196 (2011) 7931–7936. Available from: https://doi.org/10.1016/j.jpowsour.2011.05.033.

[64] D. Huang, B. Zhang, J. Bai, Y. Zhang, G. Wittstock, M. Wang, et al., Pt catalyst supported within TiO_2 mesoporous films for oxygen reduction reaction, Electrochim. Acta 130 (2014) 97–103. Available from: https://doi.org/10.1016/j.electacta.2014.02.115.

[65] I. Milošv, H.-H. Strehblow, B. Navinšek, M. Metikoš-Huković, Electrochemical and thermal oxidation of TiN coatings studied by XPS, Surf. Interface Anal. 23 (1995) 529–539. Available from: https://doi.org/10.1002/sia.740230713.

[65a] S.T. Oyama, Introduction to the chemistry of transition metal carbides and nitrides, The Chemistry of Transition Metal Carbides and Nitrides, Springer Netherlands, 1996, pp. 1–27.

[66] B. Avasarala, T. Murray, W. Li, P. Haldar, Titanium nitride nanoparticles based electrocatalysts for proton exchange membrane fuel cells, J. Mater. Chem. 19 (2009) 1803. Available from: https://doi.org/10.1039/b819006b.

[67] O.T.M. Musthafa, S. Sampath, High performance platinized titanium nitride catalyst for methanol oxidation, Chem. Commun. (2008) 67–69. Available from: https://doi.org/10.1039/b715859a.

[68] B. Avasarala, P. Haldar, On the stability of TiN-based electrocatalysts for fuel cell applications, Int. J. Hydrogen Energy 36 (2011) 3965–3974. Available from: https://doi.org/10.1016/j.ijhydene.2010.12.107.

[69] Z. Pan, Y. Xiao, Z. Fu, G. Zhan, S. Wu, C. Xiao, et al., High-performance catalyst supports for oxygen, J. Mater. Chem. A 2 (2014) 13966–13975. Available from: https://doi.org/10.1039/C4TA02402H.

[70] S. Yang, D. Young, Y. Tak, J. Kim, H. Han, J. Yu, et al., Electronic structure modification of platinum on titanium nitride resulting in enhanced catalytic activity and durability for oxygen reduction and formic acid oxidation, Appl. Catal., B 174–175 (2015) 35–42. Available from: https://doi.org/10.1016/j.apcatb.2015.02.033.

[71] Y. Dong, Y. Wu, M. Liu, J. Li, Electrocatalysis on shape-controlled titanium nitride nanocrystals for the oxygen reduction reaction, ChemSusChem (2013) 1–7. Available from: https://doi.org/10.1002/cssc.201300331.

[72] J. Kim, Y.-S. Chun, S.-K. Lee, D.-S. Lim, Improved electrode durability using a boron-doped diamond catalyst support for proton exchange membrane fuel cells, RSC Adv. 5 (2015) 1103–1108. Available from: https://doi.org/10.1039/C4RA13389G.

[73] H. Kim, M.K. Cho, J.A. Kwon, Y.H. Jeong, K.J. Lee, N.Y. Kim, et al., Highly efficient and durable TiN nanofiber electrocatalyst supports, Nanoscale 7 (2015) 18429–18434. Available from: https://doi.org/10.1039/C5NR04082E.

[74] B.S. Lee, R. Deshpande, P.A. Parilla, K.M. Jones, B. To, A.H. Mahan, et al., Crystalline WO_3 nanoparticles for highly improved electrochromic applications, Adv. Mater. 80401 (2006) 763–766. Available from: https://doi.org/10.1002/adma.200501953.

[75] J. Lee, J. Kim, T. Hyeon, Recent progress in the synthesis of porous carbon materials, Adv. Mater. 18 (2006) 2073–2094. Available from: https://doi.org/10.1002/adma.200501576.

[76] S. Supothina, P. Seeharaj, S. Yoriya, M. Sriyudthsak, Synthesis of tungsten oxide nanoparticles by acid precipitation method, Ceram. Int. 33 (2007) 931–936. Available from: https://doi.org/10.1016/j.ceramint.2006.02.007.

[77] E. Antolini, E.R. Gonzalez, Ceramic materials as supports for low-temperature fuel cell catalysts, Solid State Ionics 180 (2009) 746–763. Available from: https://doi.org/10.1016/j.ssi.2009.03.007.

[78] Y. Liu, S. Shrestha, W.E. Mustain, Synthesis of nanosize tungsten oxide and its evaluation as an electrocatalyst support for oxygen reduction in acid media, ACS Catal. 2 (2012) 456–463.

[79] N.R. Elezovic, B.M. Babic, P. Ercius, V.R. Radmilovic, L.M. Vracar, N.V. Krstajic, Synthesis and characterization Pt nanocatalysts on tungsten based supports for oxygen reduction reaction, Appl. Catal., B 125 (2012) 390–397. Available from: https://doi.org/10.1016/j.apcatb.2012.06.008.

[80] P.K. Shen, A.C.C. Tseung, Anodic oxidation of methanol on Pt/WO_3 in acidic media, J. Electrochem. Soc. 141 (1994) 3082–3089.

[81] K. Park, K. Ahn, J. Choi, Y. Nah, Y. Kim, K. Park, et al., Pt–WOx electrode structure for thin-film fuel cells, Appl. Phys. Lett. (2002) 907. Available from: https://doi.org/10.1063/1.1497707.

[82] Z. Sun, H.C. Chiu, A.C.C. Tseung, Oxygen reduction on Teflon bonded Pt/WO3/C electrode in sulfuric acid, Electrochem. Solid-State Lett. (2001) 9–12. Available from: https://doi.org/10.1149/1.1347223.

[83] R. Ganesan, J.S. Lee, An electrocatalyst for methanol oxidation based on tungsten trioxide microspheres and platinum, J. Power Sources 157 (2006) 217–221. Available from: https://doi.org/10.1016/j.jpowsour.2005.07.069.

[84] K.Y. Chen, A.C.C. Tseung, Effect of Nafion dispersion on the stability of Pt/WO_3 Electrodes, J. Electrochim. Soc. 143 (1996) 2703–2707.

[85] Y. Zhang, M. Cai, X. Sun, Carbon-coated tungsten oxide nanowires supported Pt nanoparticles for oxygen reduction, Int. J. Hydrogen Energy 37 (2011) 4633–4638. Available from: https://doi.org/10.1016/j.ijhydene.2011.05.013.

[86] B. Wickman, M. Wesselmark, C. Lagergren, G. Lindbergh, Tungsten oxide in polymer electrolyte fuel cell electrodes—a thin-film model electrode study, Electrochim. Acta 56 (2011) 9496–9503. Available from: https://doi.org/10.1016/j.electacta.2011.08.046.

[87] L. Managua, E. The, C. Rica, C. Rica, Platinum-like behavior of tungsten carbide in surface catalysis science, 547–549.

[88] H.H. Hwu, J.G. Chen, H.H. Hwu, Potential application of tungsten carbides as electrocatalysts potential application of tungsten carbides as electrocatalysts, J. Vac. Sci. Technol., A 1488 (2014). Available from: https://doi.org/10.1116/1.1582457.

[89] J.P. Bosco, K. Sasaki, M. Sadakane, W. Ueda, J.G. Chen, Synthesis and characterization of three-dimensionally ordered macroporous (3DOM) tungsten carbide: application to direct methanol fuel cells, Chem. Mater. (2010) 966–973. Available from: https://doi.org/10.1021/cm901855y.

[90] R. Wang, X. Li, H. Li, Q. Wang, H. Wang, W. Wang, et al., Highly stable and effective Pt/carbon nitride (CN_x) modified SiO_2 electrocatalyst for oxygen reduction reaction, Int. J. Hydrogen Energy 36 (2011) 5775–5781. Available from: https://doi.org/10.1016/j.ijhydene.2010.12.132.

[91] G. Cui, P. Kang, H. Meng, J. Zhao, G. Wu, Tungsten carbide as supports for Pt electrocatalysts with improved CO tolerance in methanol oxidation, J. Power Sources 196 (2011) 6125–6130. Available from: https://doi.org/10.1016/j.jpowsour.2011.03.042.

[92] M.B. Zellner, J.G. Chen, Surface science and electrochemical studies of WC and W2C PVD films as potential electrocatalysts, Catal. Today 99 (2005) 299–307. Available from: https://doi.org/10.1016/j.cattod.2004.10.004.

[93] X. Zhou, Y. Qiu, J. Yu, J. Yin, S. Gao, Tungsten carbide nanofibers prepared by electrospinning with high electrocatalytic activity for oxygen reduction, Int. J. Hydrogen Energy 36 (2011) 7398–7404. Available from: https://doi.org/10.1016/j.ijhydene.2011.03.081.

[94] M. Nie, P. Kang, M. Wu, Z. Wei, H. Meng, A study of oxygen reduction on improved Pt–WC/C electrocatalysts, J. Power Sources 162 (2006) 173–176. Available from: https://doi.org/10.1016/j.jpowsour.2006.07.015.

[95] G. Lu, J.S. Cooper, P.J. Mcginn, SECM characterization of Pt–Ru–WC and Pt–Ru–Co ternary thin film combinatorial libraries as anode electrocatalysts for PEMFC, J. Power Sources 161 (2006) 106–114. Available from: https://doi.org/10.1016/j.jpowsour.2006.04.089.

[96] R. Venkataraman, H.R. Kunz, J.M. Fenton, Development of new CO tolerant ternary anode catalysts for proton exchange membrane fuel cells, J. Electrochem. Soc. (2003) 278–284. Available from: https://doi.org/10.1149/1.1543567.

[97] Z. Shengsheng, Z.H.U. Hong, Y.U. Hongmei, H.O.U. Junbo, Y.I. Baolian, M. Pingwen, The oxidation resistance of tungsten carbide as catalyst support for proton exchange membrane fuel cells, Chin. J. Catal. 28 (2007) 109–111.

[98] H. Chhina, S. Campbell, O. Kesler, Ex situ evaluation of tungsten oxide as a catalyst support for PEMFCs, J. Electrochem. Soc. (2007) 533–539. Available from: https://doi.org/10.1149/1.2719632.

[99] H. Chhina, S. Campbell, O. Kesler, Thermal and electrochemical stability of tungsten carbide catalyst supports, J. Power Sources 164 (2007) 431–440. Available from: https://doi.org/10.1016/j.jpowsour.2006.11.003.

[100] Z. Yan, M. Cai, P.K. Shen, Nanosized tungsten carbide synthesized by a novel route at low temperature for high performance electrocatalysis, Sci. Rep. (2013) 1–7. Available from: https://doi.org/10.1038/srep01646.

[101] S. Han, H. Youn, H. Lee, J. Sung, Tungsten carbide and CNT—graphene-supported Pd electrocatalyst toward electrooxidation of hydrogen, ChemCatChem 798 (2015) 1483–1489. Available from: https://doi.org/10.1002/cctc.201500154.

[102] M. Rahsepar, M. Pakshir, P. Nikolaev, A. Safavi, K. Palanisamy, H. Kim, Tungsten carbide on directly grown multiwalled carbon nanotube as a co-catalyst for methanol oxidation, Appl. Catal., B 127 (2012) 265–272. Available from: https://doi.org/10.1016/j.apcatb.2012.08.032.

[103] M. Shao, B. Merzougui, K. Shoemaker, L. Stolar, L. Protsailo, Z.J. Mellinger, et al., Tungsten carbide modified high surface area carbon as fuel cell catalyst support, J. Power Sources 196 (2011) 7426–7434. Available from: https://doi.org/10.1016/j.jpowsour.2011.04.026.

[104] J. Zeng, C. Francia, C. Gerbaldi, V. Baglio, S. Specchia, A.S. Aricò, et al., Hybrid ordered mesoporous carbons doped with tungsten trioxide as supports for Pt electrocatalysts for methanol oxidation reaction, Electrochim. Acta 94 (2013) 80–91. Available from: https://doi.org/10.1016/j.electacta.2013.01.139.

[105] Z. Li, B. Li, Z. Liu, Z. Liu, D. Li, A tungsten carbide/iron sulfide/FePt nanocomposite supported on nitrogen-doped carbon as an efficient electrocatalyst for oxygen reduction reaction, RSC Adv. 5 (2015) 106245–106251. Available from: https://doi.org/10.1039/C5RA20895E.

[106] Y. Jiang, Y. Wang, L. Dong, J. Huang, Y. Zhang, J. Su, et al., A hybrid of titanium nitride and nitrogen-doped amorphous carbon supported on SiC as a noble metal-free electrocatalyst for oxygen reduction, Chem. Commun. (2015) 2–5. Available from: https://doi.org/10.1039/C4CC08007F.

[107] R. Li, M. Cai, X. Sun, High electrocatalytic activity of platinum nanoparticles on SnO2 nanowire-based electrodes, Electrochem. Solid-State Lett. (2007) 130–133. Available from: https://doi.org/10.1149/1.2745632.

[108] P. Zhang, S. Huang, B.N. Popov, Mesoporous tin oxide as an oxidation-resistant catalyst support for proton exchange membrane fuel cells, J. Electrochem. Soc. 157 (2010) 1163–1172. Available from: https://doi.org/10.1149/1.3442371.

[109] M. Nakada, A. Ishihara, S. Mitsushima, N. Kamiya, K. Ota, Effect of tin oxides on oxide formation and reduction of platinum particles, Electrochem. Solid-State Lett. (2007) 4–7. Available from: https://doi.org/10.1149/1.2382263.

[110] A. Sno, S. Cavaliere, I. Jimønez-morales, G. Ercolano, I. Savych, D. Jones, Highly stable PEMFC electrodes based on electrospun antimony-doped SnO_2, ChemElectroChem (2015) 1966–1973. Available from: https://doi.org/10.1002/celc.201500330.

[111] S. Cavaliere, S. Subianto, I. Savych, M. Tillard, D.J. Jones, J. Rozie, Dopant-driven nanostructured loose-tube SnO_2 architectures: alternative electrocatalyst supports for proton exchange membrane fuel cells, J. Phys. Chem. C, 117 (2013) 18298–1830.

[112] G. Ozouf, C. Beauger, Niobium- and antimony-doped tin dioxide aerogels as new catalyst supports for PEM fuel cells, J. Mater. Sci. 51 (11) (2016) 5305–5320. Available from: https://doi.org/10.1007/s10853-016-9833-7.

[113] Y. Chen, J. Wang, X. Meng, Y. Zhong, R. Li, X. Sun, et al., PteSnO_2/nitrogen-doped CNT hybrid catalysts for proton-exchange membrane fuel cells (PEMFC): effects of crystalline and amorphous SnO_2 by atomic layer deposition, J. Power Sources 238 (2013) 144–149. Available from: https://doi.org/10.1016/j.jpowsour.2013.03.093.

[114] G. Chang, M. Oyama, K. Hirao, In situ chemical reductive growth of platinum nanoparticles on indium tin oxide surfaces and their electrochemical applications, J. Phys. Chem. B, 110 (2006) 1860–1865.

[115] G. Chang, M. Oyama, K. Hirao, Seed-mediated growth of palladium nanocrystals on indium tin oxide surfaces and their applicability as modified electrodes, J. Phys. Chem. B, 110 (2006) 20362–20368.

[116] Y. Wang, D.P. Wilkinson, J. Zhang, Noncarbon support materials for polymer electrolyte membrane fuel cell electrocatalysts, Chem. Rev. 111 (2011) 7625–7651.

[117] X. Wang, J.S. Lee, Q. Zhu, J. Liu, Y. Wang, S. Dai, Ammonia-treated ordered mesoporous carbons as catalytic materials for oxygen reduction reaction, Chem. Mater. 22 (2010) 2178–2180. Available from: https://doi.org/10.1021/cm100139d.

[118] D. Long, W. Li, L. Ling, J. Miyawaki, I. Mochida, S.H. Yoon, Preparation of nitrogen-doped graphene sheets by a combined chemical and hydrothermal reduction of graphene oxide, Langmuir 26 (2010) 16096–16102. Available from: https://doi.org/10.1021/la102425a.

[119] Z. Yang, Z. Yao, G. Li, G. Fang, H. Nie, Z. Liu, et al., Sulfur-doped graphene as an efficient metal-free cathode catalyst for oxygen reduction, ACS Nano 6 (2012) 205–211. Available from: https://doi.org/10.1021/nn203393d.

[120] D. Deng, X. Pan, L. Yu, Y. Cui, Y. Jiang, J. Qi, et al., Toward N-doped graphene via solvothermal synthesis, Chem. Mater. 23 (2011) 1188–1193. Available from: https://doi.org/10.1021/cm102666r.

[121] Q. Wen, S. Wang, J. Yan, L. Cong, Y. Chen, H. Xi, Porous nitrogen-doped carbon nanosheet on graphene as metal-free catalyst for oxygen reduction reaction in air-cathode microbial fuel cells, Bioelectrochemistry 95 (2014) 23–28. Available from: https://doi.org/10.1016/j.bioelechem.2013.10.007.

[122] A. Eftekhari, Z. Fan, Ordered mesoporous carbon and its applications for electrochemical energy storage and conversion, Mater. Chem. Front. 1 (2017) 1001–1027. Available from: https://doi.org/10.1039/C6QM00298F.

[123] J. Wintterlin, M.L. Bocquet, Graphene on metal surfaces, Surf. Sci. 603 (2009) 1841–1852. Available from: https://doi.org/10.1016/j.susc.2008.08.037.

[124] M.D. Stoller, S. Park, Z. Yanwu, J. An, R.S. Ruoff, Graphene-based ultracapacitors, Nano Lett. 8 (2008) 3498–3502. Available from: https://doi.org/10.1021/nl802558y.

[125] Z.-J. Lu, S.-J. Bao, Y.-T. Gou, C.-J. Cai, C.-C. Ji, M.-W. Xu, et al., Nitrogen-doped reduced-graphene oxide as an efficient metal-free electrocatalyst for oxygen reduction in fuel cells, RSC Adv. 3 (2013) 3990. Available from: https://doi.org/10.1039/c3ra22161j.

[126] D. Guo, R. Shibuya, C. Akiba, S. Saji, T. Kondo, J. Nakamura, Active sites of nitrogen-doped carbon materials for oxygen reduction reaction clarified using model catalysts, Science 351 (2016) 361–365. Available from: https://doi.org/10.1126/science.aad0832.

[127] W.Y. Wong, W.R.W. Daud, A.B. Mohamad, A.A.H. Kadhum, K.S. Loh, E.H. Majlan, Recent progress in nitrogen-doped carbon and its composites as electrocatalysts for fuel cell applications, Int. J. Hydrogen Energy 38 (2013) 9370–9386. Available from: https://doi.org/10.1016/j.ijhydene.2012.12.095.

[128] A.L. Dicks, The role of carbon in fuel cells, J. Power Sources 156 (2006) 128–141. Available from: https://doi.org/10.1016/j.jpowsour.2006.02.054.

[129] Z. Peng, J. Wu, H. Yang, Synthesis and oxygen reduction electrocatalytic property of platinum hollow and platinum-on-silver nanoparticles, Chem. Mater. 22 (2010) 1098–1106. Available from: https://doi.org/10.1021/cm902218j.

[130] J. Dodelet, B.S. Sun, Controlled growth of Pt nanowires on carbon nanospheres and their enhanced performance as electrocatalysts in PEM fuel cells, Adv. Mater. (2008) 3900–3904. Available from: https://doi.org/10.1002/adma.200800491.

[131] S. Zhang, S. Chen, Enhanced-electrocatalytic activity of Pt nanoparticles supported on nitrogen-doped carbon for the oxygen reduction reaction, J. Power Sources 240 (2013) 60–65. Available from: https://doi.org/10.1016/j.jpowsour.2013.03.149.

[132] C. Zhang, N. Mahmood, H. Yin, F. Liu, Y. Hou, Synthesis of phosphorus-doped graphene and its multifunctional applications for oxygen reduction reaction and lithium ion batteries, Adv. Mater. 25 (2013) 4932–4937. Available from: https://doi.org/10.1002/adma.201301870.

[133] G. Bae, D.H. Youn, S. Han, J.S. Lee, The role of nitrogen in a carbon support on the increased activity and stability of a Pt catalyst in electrochemical hydrogen oxidation, Carbon 51 (2013) 274–281. Available from: https://doi.org/10.1016/j.carbon.2012.08.054.

[134] H. Lv, N. Cheng, T. Peng, M. Pan, S. Mu, High stability platinum electrocatalysts with zirconia–carbon hybrid supports, J. Mater. Chem. 22 (2012) 1135–1141. Available from: https://doi.org/10.1039/C1JM14076K.

[135] K. Kakaei, Electrochemical characteristics and performance of platinum nanoparticles supported by Vulcan/polyaniline for oxygen reduction in PEMFC, Fuel Cells 12 (2012) 939–945. Available from: https://doi.org/10.1002/fuce.201200053.

[136] F. Memioğlu, A. Bayrakçeken, T. Öznülüer, M. Ak, Synthesis and characterization of polypyrrole/carbon composite as a catalyst support for fuel cell applications, Int. J. Hydrogen Energy 37 (2012) 16673–16679. Available from: https://doi.org/10.1016/j.ijhydene.2012.02.086.

[137] S.M. Senthil Kumar, J. Soler Herrero, S. Irusta, K. Scott, The effect of pretreatment of Vulcan XC-72R carbon on morphology and electrochemical oxygen reduction kinetics of supported Pd nano-particle in acidic electrolyte, J. Electroanal. Chem. 647 (2010) 211–221. Available from: https://doi.org/10.1016/j.jelechem.2010.05.021.

[138] S. Sharma, B.G. Pollet, Support materials for PEMFC and DMFC electrocatalysts—a review, J. Power Sources 208 (2012) 96–119. Available from: https://doi.org/10.1016/j.jpowsour.2012.02.011.

[139] S. Shahgaldi, J. Hamelin, Improved carbon nanostructures as a novel catalyst support in the cathode side of PEMFC: a critical review, Carbon 94 (2015) 705–728. Available from: https://doi.org/10.1016/j.carbon.2015.07.055.

[140] M.S. Saha, A. Kundu, Functionalizing carbon nanotubes for proton exchange membrane fuel cells electrode, J. Power Sources 195 (2010) 6255–6261. Available from: https://doi.org/10.1016/j.jpowsour.2010.04.015.

[141] B.G. Pollet, The use of ultrasound for the fabrication of fuel cell materials, Int. J. Hydrogen Energy 35 (2010) 11986–12004. Available from: https://doi.org/10.1016/j.ijhydene.2010.08.021.

[142] C. Du, M. Chen, X. Cao, G. Yin, P. Shi, A novel CNT@SnO_2 core-sheath nanocomposite as a stabilizing support for catalysts of proton exchange membrane fuel cells, Electrochem. Commun. 11 (2009) 496–498. Available from: https://doi.org/10.1016/j.elecom.2008.12.034.

[143] L.M. Reddy, S. Ramaprabhu, Pt/SWNT-Pt/C nanocomposite electrocatalysts for proton-exchange membrane fuel cells, J. Phys. Chem. C 111 (2007) 16138–16146.

[144] G. Girishkumar, M. Rettker, R. Underhile, D. Binz, K. Vinodgopal, P. Mcginn, et al., Single-wall carbon nanotube-based proton exchange membrane assembly for hydrogen fuel cells, Langmuir (2005) 8487–8494. Available from: https://doi.org/10.1021/la051499j.

[145] Z. Tang, C.K. Poh, K.K. Lee, Z. Tian, D.H.C. Chua, J. Lin, Enhanced catalytic properties from platinum nanodots covered carbon nanotubes for proton-exchange membrane fuel cells, J. Power Sources 195 (2010) 155–159. Available from: https://doi.org/10.1016/j.jpowsour.2009.06.105.

[146] Y. Shen, Z. Xia, Y. Wang, C.K. Poh, J. Lin, Pt coated vertically aligned carbon nanotubes as electrodes for proton exchange membrane fuel cells, Procedia Eng. 93 (2014) 34–42. Available from: https://doi.org/10.1016/j.proeng.2013.11.037.

[147] E. Das, A.B. Yurtcan, Effect of carbon ratio in the polypyrrole/carbon composite catalyst support on PEM fuel cell performance, Int. J. Hydrogen Energy 41 (2016) 13171–13179. Available from: https://doi.org/10.1016/j.ijhydene.2016.05.167.

[148] D. Kaewsai, P. Piumsomboon, K. Pruksathorn, M. Hunsom, Synthesis of polyaniline-wrapped carbon nanotube-supported PtCo catalysts for proton exchange membrane fuel cells: activity and stability tests, RSC Adv. 7 (2017) 20801–20810. Available from: https://doi.org/10.1039/C7RA01514C.

[149] H. Zhao, L. Li, J. Yang, Y. Zhang, Nanostructured polypyrrole/carbon composite as Pt catalyst support for fuel cell applications, J. Power Sources 184 (2008) 375–380. Available from: https://doi.org/10.1016/j.jpowsour.2008.03.024.

[150] D. He, C. Zeng, C. Xu, N. Cheng, H. Li, S. Mu, et al., Polyaniline-functionalized carbon nanotube supported platinum catalysts, Langmuir 27 (2011) 5582–5588. Available from: https://doi.org/10.1021/la2003589.

[151] Y. Chen, J. Wang, H. Liu, M.N. Banis, R. Li, X. Sun, et al., Nitrogen doping effects on carbon nanotubes and the origin of the enhanced electrocatalytic activity of supported Pt for proton-exchange membrane fuel cells, J. Phys. Chem. C 115 (2011) 3769–3776. Available from: https://doi.org/10.1021/jp108864y.

[152] M.N. Banis, S. Sun, X. Meng, Y. Zhang, Z. Wang, R. Li, et al., $TiSi_2O_x$ coated N-doped carbon nanotubes as Pt catalyst support for the oxygen reduction reaction in PEMFCs, J. Phys. Chem. C 117 (2013) 15457–15467. Available from: https://doi.org/10.1021/jp3118874.

[153] D. Long, W. Li, W. Qiao, J. Miyawaki, S.-H. Yoon, I. Mochida, et al., Partially unzipped carbon nanotubes as a superior catalyst support for PEM fuel cells, Chem. Commun. 47 (2011) 9429–9431. Available from: https://doi.org/10.1039/c1cc13488d.

[154] A. Morozan, S. Campidelli, A. Filoramo, B. Jousselme, S. Palacin, Catalytic activity of cobalt and iron phthalocyanines or porphyrins supported on different carbon nanotubes towards oxygen reduction reaction, Carbon 49 (2011) 4839–4847. Available from: https://doi.org/10.1016/j.carbon.2011.07.004.

[155] Y. Liang, H. Wang, P. Diao, W. Chang, G. Hong, et al., Oxygen reduction electrocatalyst based on strongly coupled cobalt oxide, J. Am. Chem. Soc. 134 (38) (2012) 15849–15857.

[156] B.P. Vinayan, R.I. Jafri, R. Nagar, N. Rajalakshmi, K. Sethupathi, S. Ramaprabhu, Catalytic activity of platinum–cobalt alloy nanoparticles decorated functionalized multiwalled carbon nanotubes for oxygen reduction reaction in PEMFC, Int. J. Hydrogen Energy 37 (2012) 412–421. Available from: https://doi.org/10.1016/j.ijhydene.2011.09.069.

[157] M. Tsuji, M. Kubokawa, R. Yano, N. Miyamae, T. Tsuji, M.S. Jun, et al., Fast preparation of PtRu catalysts supported on carbon nanofibers by the microwave-polyol method and their application to fuel cells, Langmuir 23 (2007) 387–390. Available from: https://doi.org/10.1021/la062223u.

[158] S. Li, C. Chen, K. Fu, R. White, C. Zhao, P.D. Bradford, et al., Nanosized Ge@CNF, Ge@C@CNF and Ge@CNF@C composites via chemical vapour deposition method for use in advanced lithium-ion batteries, J. Power Sources 253 (2014) 366–372. Available from: https://doi.org/10.1016/j.jpowsour.2013.12.017.

[159] X. Tang, et al., Mass-transport-controlled, large-area, uniform deposition of carbon nanofibers and their application in gas diffusion layers of fuel cells, Nanoscale 7 (2015) 7971–7979. Available from: https://doi.org/10.1039/b000000x.

[160] Z.-J. Fan, J. Yan, T. Wei, G.-Q. Ning, L.-J. Zhi, J.-C. Liu, et al., Nanographene-constructed carbon nanofibers grown on graphene sheets by chemical vapor deposition: high-performance anode materials for lithium ion batteries, ACS Nano 5 (2011) 2787–2794. Available from: https://doi.org/10.1021/nn200195k.

[161] D. Sebastián, A. García, I. Suelves, R. Moliner, M. Jesús, V. Baglio, et al., Enhanced oxygen reduction activity and durability of Pt catalysts supported on carbon nanofibers, Appl. Catal., B 115–116 (2012) 269–275. Available from: https://doi.org/10.1016/j.apcatb.2011.12.041.

[162] W. Li, M. Waje, Z. Chen, P. Larsen, Y. Yan, Platinum nanoparticles supported on stacked-cup carbon nanofibers as electrocatalysts for proton exchange membrane fuel cell, Carbon 48 (2010) 995–1003. Available from: https://doi.org/10.1016/j.carbon.2009.11.017.

[163] R. Padmavathi, D. Sangeetha, Synthesis and characterization of electrospun carbon nanofiber supported Pt catalyst for fuel cells, Electrochim. Acta 112 (2013) 1–13. Available from: https://doi.org/10.1016/j.electacta.2013.08.078.

[164] A. Guha, W. Lu, T.A. Zawodzinski, D.A. Schiraldi, Surface-modified carbons as platinum catalyst support for PEM fuel cells, Carbon 45 (2007) 1506–1517. Available from: https://doi.org/10.1016/j.carbon.2007.03.023.

[165] R.S. Zhong, Y.H. Qin, D.F. Niu, X.S. Zhang, X.G. Zhou, S.G. Sun, et al., Effect of carbon nanofiber surface groups on oxygen reduction reaction of supported Pt electrocatalyst, Electrochim. Acta 89 (2013) 157–162. Available from: https://doi.org/10.1016/j.electacta.2012.11.007.

[166] J.S. Zheng, M.X. Wang, X.S. Zhang, Y.X. Wu, P. Li, X.G. Zhou, et al., Platinum/carbon nanofiber nanocomposite synthesized by electrophoretic deposition as electrocatalyst for oxygen reduction, J. Power Sources 175 (2008) 211–216. Available from: https://doi.org/10.1016/j.jpowsour.2007.09.058.

[167] P. Zamani, D. Higgins, F. Hassan, G. Jiang, J. Wu, S. Abureden, et al., Electrospun iron-polyaniline-polyacrylonitrile derived nanofibers as non-precious oxygen reduction reaction catalysts for PEM fuel cells, Electrochim. Acta 139 (2014) 111–116. Available from: https://doi.org/10.1016/j.electacta.2014.07.007.

[168] G. Ren, X. Lu, Y. Li, Y. Zhu, L. Dai, L. Jiang, Porous core−shell Fe_3C embedded N-doped carbon nanofibers as an effective electrocatalysts for oxygen reduction reaction, ACS Appl. Mater. Interfaces 8 (2016) 4118−4125. Available from: https://doi.org/10.1021/acsami.5b11786.

[169] Q. Guo, D. Zhao, S. Liu, S. Chen, M. Hanif, H. Hou, Free-standing nitrogen-doped carbon nanotubes at electrospun carbon nanofibers composite as an efficient electrocatalyst for oxygen reduction, Electrochim. Acta 138 (2014) 318−324. Available from: https://doi.org/10.1016/j.electacta.2014.06.120.

[170] Y. Jiang, J. Zhang, Y.-H. Qin, D.-F. Niu, X.-S. Zhang, L. Niu, et al., Ultrasonic synthesis of nitrogen-doped carbon nanofibers as platinum catalyst support for oxygen reduction, J. Power Sources 196 (2011) 9356−9360. Available from: https://doi.org/10.1016/j.jpowsour.2011.07.036.

[171] J.S. Zheng, X.Z. Wang, J.L. Qiao, D.J. Yang, B. Li, P. Li, et al., Ir−V nanoparticles supported on microstructure controlled carbon nanofibers as electrocatalyst for oxygen reduction reaction, Electrochem. Commun. 12 (2010) 27−31. Available from: https://doi.org/10.1016/j.elecom.2009.10.028.

[172] F. Yuan, H. Ryu, The synthesis, characterization, and performance of carbon nanotubes and carbon nanofibres with controlled size and morphology as a catalyst support material for a polymer electrolyte membrane fuel cell, Nanotechnology 15 (2004) S596−S602. Available from: https://doi.org/10.1088/0957-4484/15/10/017.

[173] K.K. Karthikeyan, P. Biji, A novel biphasic approach for direct fabrication of highly porous, flexible conducting carbon nanofiber mats from polyacrylonitrile (PAN)/$NaHCO_3$ nanocomposite, Microporous Mesoporous Mater. 224 (2016) 372−383. Available from: https://doi.org/10.1016/j.micromeso.2015.12.055.

[174] D. Shin, B. Jeong, B.S. Mun, H. Jeon, H.J. Shin, J. Baik, et al., On the origin of electrocatalytic oxygen reduction reaction on electrospun nitrogen—carbon species, J. Phys. Chem. C 117 (2013) 11619−11624. Available from: https://doi.org/10.1021/jp401186a.

[175] E. Lohrasbi, M. Javanbakht, S.A. Mozaffari, Synthesis of graphene-supported PtCoFe alloy with different thermal treatment procedures as highly active oxygen reduction reaction electrocatalysts for proton exchange membrane fuel cells, Ind. Eng. Chem. Res. 55 (2016) 9154−9163. Available from: https://doi.org/10.1021/acs.iecr.6b00980.

[176] N. Shaari, S.K. Kamarudin, Graphene in electrocatalyst and proton conducting membrane in fuel cell applications: an overview, Renewable Sustainable Energy Rev. 69 (2017) 862−870. Available from: https://doi.org/10.1016/j.rser.2016.07.044.

[177] C.T. Hsieh, J.M. Wei, J.S. Lin, W.Y. Chen, Pulse electrodeposition of Pt nanocatalysts on graphene-based electrodes for proton exchange membrane fuel cells, Catal. Commun. 16 (2011) 220−224. Available from: https://doi.org/10.1016/j.catcom.2011.09.030.

[178] M. Cattelan, S. Agnoli, M. Favaro, D. Garoli, F. Romanato, M. Meneghetti, et al., Microscopic view on a chemical vapor deposition route to boron-doped graphene nanostructures, Chem. Mater. 25 (2013) 1490−1495. Available from: https://doi.org/10.1021/cm302819b.

[179] L.S. Panchakarla, K.S. Subrahmanyam, S.K. Saha, A. Govindaraj, H.R. Krishnamurthy, U.V. Waghmare, et al., Synthesis, structure, and properties of boron- and nitrogen-doped graphene, Adv. Mater. 21 (2009) 4726−4730. Available from: https://doi.org/10.1002/adma.200901285.

[180] C.H. Choi, M.W. Chung, H.C. Kwon, S.H. Park, S.I. Woo, B, N- and P, N-doped graphene as highly active catalysts for oxygen reduction reactions in acidic media, J. Mater. Chem. A 1 (2013) 3694. Available from: https://doi.org/10.1039/c3ta01648j.

[181] C. Liang, Z. Li, S. Dai, Mesoporous carbon materials: synthesis and modification, Angew. Chem. Int. Ed. Engl. 47 (2008) 3696−3717. Available from: https://doi.org/10.1002/anie.200702046.

[182] K.L. Yeung, W. Han, Zeolites and mesoporous materials in fuel cell applications, Catal. Today 236 (2014) 182−205. Available from: https://doi.org/10.1016/j.cattod.2013.10.022.

[183] H. Chang, S.H. Joo, C. Pak, Synthesis and characterization of mesoporous carbon for fuel cell applications, J. Mater. Chem. 17 (2007) 3078. Available from: https://doi.org/10.1039/b700389g.

[184] W. Xu, S. Tao, Recent progress in electrocatalysts with mesoporous structures for application in polymer electrolyte membrane fuel cells, J. Mater. Chem. A 4 (2016) 16272−16287. Available from: https://doi.org/10.1039/C6TA05304A.

[185] J.S. Yu, S. Kang, S.B. Yoon, G. Chai, Fabrication of ordered uniform porous carbon networks and their application to a catalyst supporter, J. Am. Chem. Soc. 124 (2002) 9382−9383. Available from: https://doi.org/10.1021/ja0203972.

[185a] S.H. Joo, S.J. Choi, I. Oh, J. Kwak, Z. Liu, O. Terasaki, et al., Correction: ordered nanoporous arrays of carbon supporting high dispersions of platinum nanoparticles, Nature 414 (2001). Available from: https://doi.org/10.1038/35106621. 470.

[186] J. Ding, K.Y. Chan, J. Ren, F.S. Xiao, Platinum and platinum-ruthenium nanoparticles supported on ordered mesoporous carbon and their electrocatalytic performance for fuel cell reactions, Electrochim. Acta 50 (2005) 3131−3141. Available from: https://doi.org/10.1016/j.electacta.2004.11.064.

[187] P. Liu, J. Kong, Y. Liu, Q. Liu, H. Zhu, Graphitic mesoporous carbon based on aromatic polycondensation as catalyst support for oxygen reduction reaction, J. Power Sources 278 (2015) 522−526. Available from: https://doi.org/10.1016/j.jpowsour.2014.12.122.

[188] F.A. Viva, M.M. Bruno, E.A. Franceschini, Y.R.J. Thomas, G. Ramos Sanchez, O. Solorza-Feria, et al., Mesoporous carbon as Pt support for PEM fuel cell, Int. J. Hydrogen Energy 39 (2014) 8821−8826. Available from: https://doi.org/10.1016/j.ijhydene.2013.12.027.

[189] D. Banham, F. Feng, K. Pei, S. Ye, V. Birss, Effect of carbon support nanostructure on the oxygen reduction activity of Pt/C catalysts, J. Mater. Chem. A 1 (2013) 2812. Available from: https://doi.org/10.1039/c2ta00868h.

[190] E.P. Lee, Ḱ.Z. Peng, Ḱ.W. Chen, S. Chen, H. Yang, Y. Xia, Electrocatalytic properties of Pt nanowires supported on Pt and W gauzes, ACS Nano 2 (2008) 2167−2173.

[191] C.Y. Ahn, J.Y. Cheon, S.H. Joo, J. Kim, Effects of ionomer content on Pt catalyst/ordered mesoporous carbon support in polymer electrolyte membrane fuel cells, J. Power Sources 222 (2013) 477−482. Available from: https://doi.org/10.1016/jjpowsour.2012.09.012.

[191a] S.-H. Liu, C.-C. Chiang, M.-T. Wu, S.-B. Liu, Electrochemical activity and durability of platinum nanoparticles supported on ordered mesoporous carbons for oxygen reduction reaction, Int. J. Hydrogen Energy 35 (2010) 8149−8154. Available from: https://doi.org/10.1016/j.ijhydene.2009.12.183.

[192] K.N. Sultana, A.L. Fadhel, V.G. Deshmane, S. Ilias, Novel method for synthesis of electrocatalyst via catalytic graphitization of ordered mesoporous carbon for PEMFC application, Sep. Sci. Technol. (2017) 6395. Available from: https://doi.org/10.1080/01496395.2017.1290657.

[193] J.Y. Cheon, T. Kim, Y. Choi, H.Y. Jeong, M.G. Kim, Y.J. Sa, et al., Ordered mesoporous porphyrinic carbons with very high electrocatalytic activity for the oxygen reduction reaction, Sci. Rep. (2013) 1−8. Available from: https://doi.org/10.1038/srep02715.

[194] T.A. Ivandini, R. Sato, Y. Makide, A. Fujishima, Y. Einaga, Electrochemical detection of arsenic(III) using iridium-implanted boron-doped diamond electrodes, Anal. Chem. 78 (2006) 6291−6298. Available from: https://doi.org/10.1021/ac0519514.

[195] X. Lu, J. Hu, J.S. Foord, Q. Wang, Electrochemical deposition of Pt−Ru on diamond electrodes for the electrooxidation of methanol, J. Electroanal. Chem. 654 (2011) 38−43. Available from: https://doi.org/10.1016/j.jelechem.2011.01.034.

[196] J.H.T. Luong, K.B. Male, J.D. Glennon, Boron-doped diamond electrode: synthesis, characterization, functionalization and analytical applications, Analyst 134 (2009) 1965. Available from: https://doi.org/10.1039/b910206j.

[196a] G.R. Salazar-Banda, K.I.B. Eguiluz, L.A. Avaca, Boron-doped diamond powder as catalyst support for fuel cell applications, Electrochem. Commun. 9 (2007) 59−64. Available from: https://doi.org/10.1016/j.elecom.2006.08.038.

[196b] G.R. Salazar-Banda, H.B. Suffredini, L.A. Avaca, S.A.S. Machado, Methanol and ethanol electro-oxidation on Pt−SnO_2 and Pt−Ta_2O_5 sol−gel-modified boron-doped diamond surfaces, Mater. Chem. Phys. 117 (2009) 434−442. Available from: https://doi.org/10.1016/j.matchemphys.2009.06.027.

[196c] G.M. Swain, R. Ramesham, The electrochemical activity of boron-doped polycrystalline diamond thin film electrodes, Anal. Chem 65 (1993) 345−351. Available from: https://doi.org/10.1021/ac00052a00.

[197] L. La-Torre-Riveros, K. Soto, M.A. Scibioh, C.R. Cabrera, Electrophoretically fabricated diamond nanoparticle-based electrodes,

J. Electrochem. Soc. 157 (2010) B831. Available from: https://doi.org/10.1149/1.3374403.

[198] S. Maass, F. Finsterwalder, G. Frank, R. Hartmann, C. Merten, Carbon support oxidation in PEM fuel cell cathodes, J. Power Sources 176 (2008) 444–451. Available from: https://doi.org/10.1016/j.jpowsour.2007.08.053.

FURTHER READING

M.J. Allen, V.C. Tung, R.B. Kaner, Honeycomb carbon: a review of graphene, Chem. Rev. 110 (2010) 132–145. Available from: https://doi.org/10.1021/cr900070d.

A.K. Geim, K.S. Novoselov, The rise of graphene, Nat. Mater. 207 (6) (2007) 183–191. Availablefrom: https://doi.org/10.1038/nmat1849.

A.A. Balandin, S. Ghosh, W. Bao, I. Calizo, D. Teweldebrhan, F. Miao, et al., Superior thermal conductivity of single-layer graphene, Nano Lett. 8 (2008) 902–907. Available from: https://doi.org/10.1021/nl0731872.

C. Berger, Z. Song, T. Li, X. Li, A.Y. Ogbazghi, R. Feng, et al., Ultrathin epitaxial graphite: 2D electron gas properties and a route toward graphene-based nanoelectronics, J. Phys. Chem. B 108 (2004) 19912–19916. Available from: https://doi.org/10.1021/jp040650f.

J. Campos-Delgado, Y.A. Kim, T. Hayashi, A. Morelos-Gómez, M. Hofmann, H. Muramatsu, et al., Thermal stability studies of CVD-grown graphene nanoribbons: defect annealing and loop formation, Chem. Phys. Lett. 469 (2009) 177–182. Available from: https://doi.org/10.1016/j.cplett.2008.12.082.

L. Dai, Y. Xue, L. Qu, H. Choi, J. Baek, Metal-free catalysts for oxygen reduction reaction, Chem. Rev. 115 (11) (2014) 4823–4892. Available from: https://doi.org/10.1021/cr5003563.

E. Higuchi, K. Okamoto, K. Miyatake, H. Uchida, M. Watanabe, Gas diffusion electrodes for polymer electrolyte fuel cell using sulfonated polyimide, Res. Chem. Intermed. 32 (2006) 533–542. Available from: https://doi.org/10.1163/156856706777973781.

K. Jiang, Q. Jia, M. Xu, D. Wu, L. Yang, G. Yang, et al., A novel non-precious metal catalyst synthesized via pyrolysis of polyaniline-coated tungsten carbide particles for oxygen reduction reaction, J. Power Sources 219 (2012) 249–252. Available from: https://doi.org/10.1016/j.jpowsour.2012.07.056.

R. Li, X. Sun, Composite of Pt–Ru supported SnO2 nanowires grown on carbon paper for electrocatalytic oxidation of methanol, Electrochem. Commun. 9 (2007) 2229–2234. Available from: https://doi.org/10.1016/j.elecom.2007.06.032.

Lin, J.F.; Kamavaram, V.; Kannan, A.M. Synthesis and characterization of carbon nanotubes supported platinum nanocatalyst for proton exchange membrane fuel cells. J. Power Sources 2010;195; 466–470.

J. Liu, D. Takeshi, K. Sasaki, S.M. Lyth, Defective graphene foam: a platinum catalyst support for PEMFCs, J. Electrochem. Soc. 161 (2014) F838–F844. Available from: https://doi.org/10.1149/2.0231409jes.

Q. Liu, T. Fujigaya, N. Nakashima, Graphene unrolled from "cup-stacked" carbon nanotubes, Carbon 50 (2012) 5421–5428. Available from: https://doi.org/10.1016/j.carbon.2012.07.028.

Y. Lu, Y. Jiang, H. Wu, W. Chen, Nano-PtPd cubes on graphene exhibit enhanced activity and durability in methanol electrooxidation after CO stripping-cleaning, J. Phys. Chem. C 117 (2013) 2926–2938. Available from: https://doi.org/10.1021/jp3116726.

A. Peigney, C. Laurent, E. Flahaut, R.R. Bacsa, A. Rousset, Specific surface area of carbon nanotubes and bundles of carbon nanotubes, Carbon 39 (2001) 507–514. Available from: https://doi.org/10.1016/S0008-6223(00)00155-X.

V. Raghuveer, B. Viswanathan, Synthesis, characterization and electrochemical studies of Ti-incorporated tungsten trioxides as platinum support for methanol oxidation, J. Power Sources 144 (2005) 1–10. Available from: https://doi.org/10.1016/j.jpowsour.2004.11.033.

Y. Shi, K.K. Kim, A. Reina, M. Hofmann, L.J. Li, J. Kong, Work function engineering of graphene electrode via chemical doping, ACS Nano 4 (2010) 2689–2694. Available from: https://doi.org/10.1021/nn1005478.

X. Wang, L. Zhi, K. Müllen, Transparent, conductive graphene electrodes for dye-sensitized solar cells, Nano Lett. 8 (2008) 323–327. Available from: https://doi.org/10.1021/nl072838r.

Y. Wang, Y. Shao, D.W. Matson, J. Li, Y. Lin, Nitrogen-doped graphene and its biosensing, ACS Nano 4 (2010) 1790–1798. Available from: https://doi.org/10.1063/1.4870424.

J.-S. Zheng, X.-S. Zhang, P. Li, J. Zhu, X.-G. Zhou, W.-K. Yuan, Effect of carbon nanofiber microstructure on oxygen reduction activity of supported palladium electrocatalyst, Electrochem. Commun. 9 (2007) 895–900. Available from: https://doi.org/10.1016/j.elecom.2006.12.006.